

Projected material requirements for the global electricity infrastructure – generation, transmission and storage

S. Deetman^{1,3}, H.S. de Boer², M. Van Engelenburg¹, E. van der Voet¹, D.P. van Vuuren^{2,3}

¹Institute of Environmental Sciences, Leiden University, Leiden, the Netherlands

²PBL Netherlands Environmental Assessment Agency, The Hague, The Netherlands

³Copernicus Institute for Sustainable Development, Utrecht University, Utrecht, The Netherlands

Number of pages: 38

Number of figures: 24

Number of tables: 16

1. IMAGE Region definitions.....	2
2. Detailed model assumptions on generation, transmission and storage	3
2.1 Electricity generation capacity.....	3
2.2 Electricity Transmission, the Grid	5
2.2.1 Grid Lengths	5
2.2.2 Undergrounding of power lines	8
2.2.3 Substations and Transformers.....	8
2.2.4 Lifetime of Grid Elements	8
2.2.5 Material Intensities of Grid Elements	9
2.3 Electricity Storage.....	9
2.3.1 Electricity Storage Demand.....	9
2.3.2. Pumped Hydro storage	10
2.3.3. Electricity Storage in Electric Vehicles	10
2.3.4. Dedicated storage demand.....	12
2.3.5. Market Shares of storage technologies	13
3. Comparing outcomes.....	18
4. Sensitivity Analysis	19
4.1 Alternative assumptions on drivers: transmission and storage.....	19
4.2 Alternative assumptions on material intensities	22
4.3. Results of the Sensitivity Analysis	23
5. Model Code.....	25
6. Detailed results	26
References to the Supplementary Information.....	34

1. IMAGE Region definitions

The regional classification used in the main text and the IMAGE model distinguish 26 global regions, which can be seen in Figure S.1, below. We've also indicated which regions are grouped under 'fast developing' with a 1, and 'steady developed' regions with a 2, according to the identified regional typologies used in the main text. Buildings in Greenland & Antarctica are not taken into account.

The 26 world regions in IMAGE 3.0

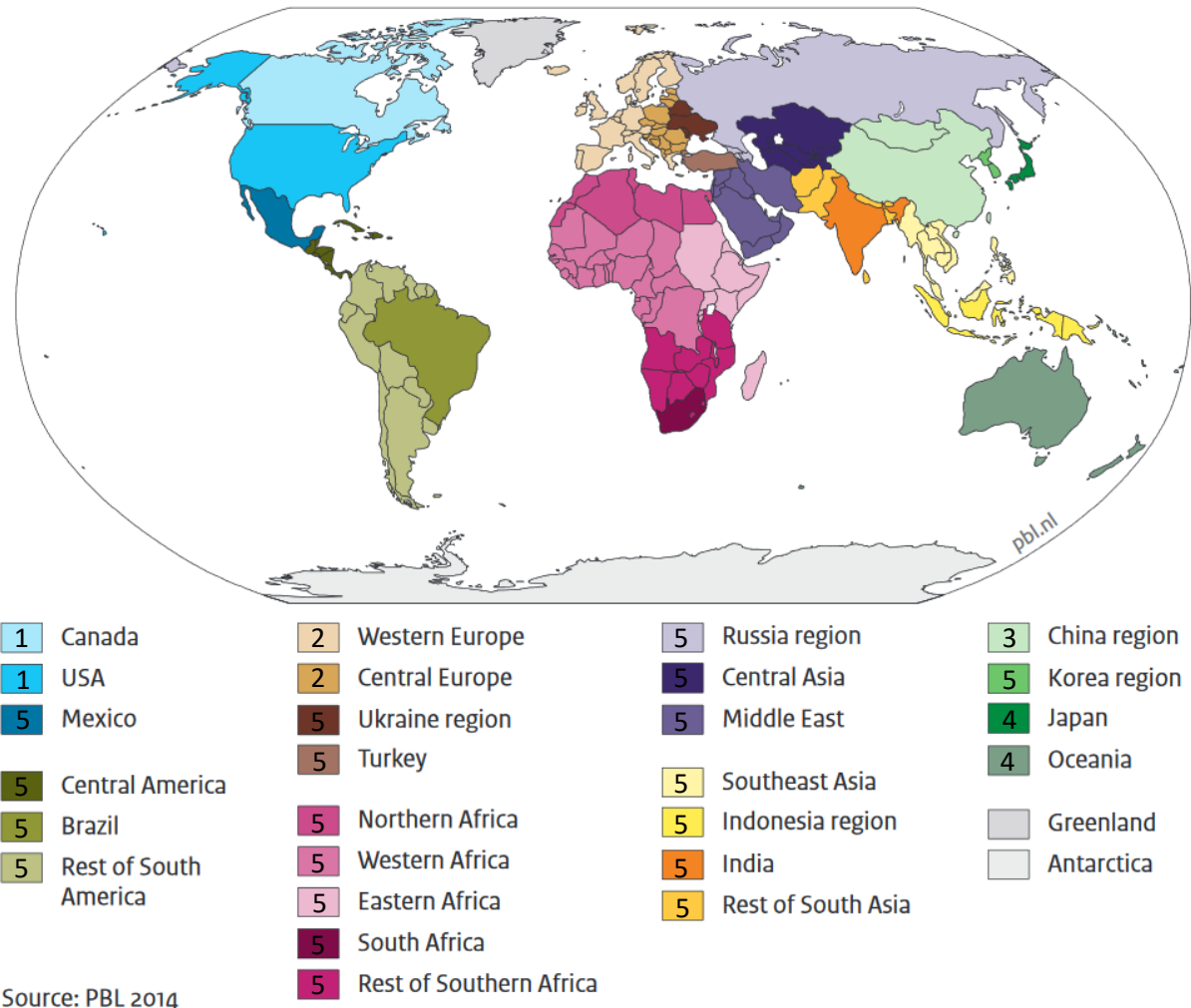


Figure S.1. The 26 world regions in IMAGE 3.0. Source: Stehfest et al. [1], reproduced with permission of the editor. In Figure S.2 and S.8, regions tagged with a 1 are part of the group classified as 'North America', 2 refers to 'Europe', 3 is China, 4 the sum of Japan and Oceania and all regions tagged with 5 are displayed as part of Rest of the World.

2. Detailed model assumptions on generation, transmission and storage

2.1 Electricity generation capacity

The development of generation capacity is one of two main drivers of our material model and is given as an output of the IMAGE/TIMER model [2] based on the SSP2 scenario used in this study [3]. Corresponding to the total global generation capacity as provided in the main text (Figure 3), Figure S.2 provides some more regional detail with respect to the development of generation capacities by technology.

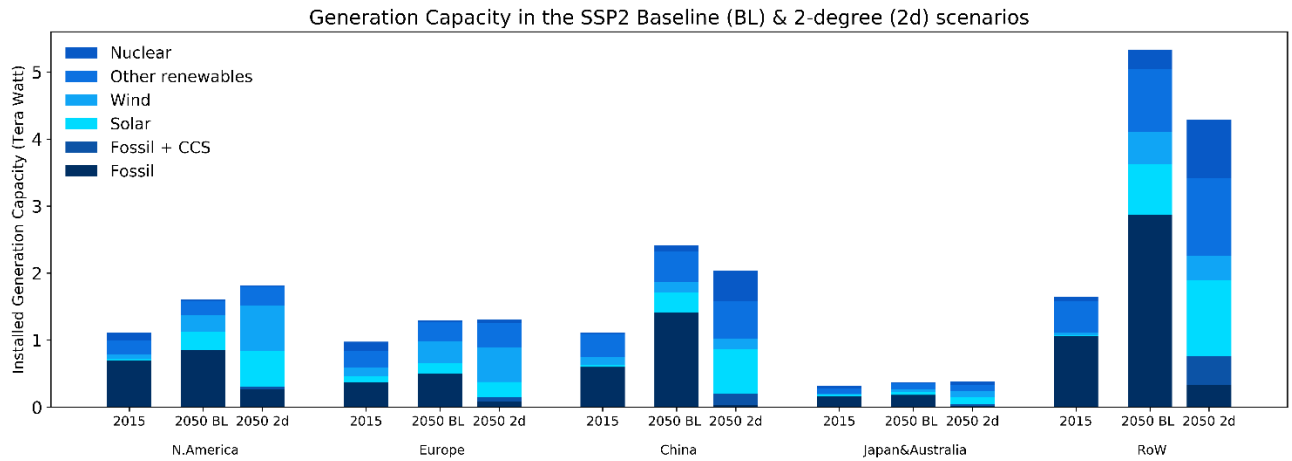


Figure S.2. Electricity Generation Capacity in the SSP2 Baseline and 2-degree scenarios according to the IMAGE model [2], [3]. More information on assumptions underlying the SSP scenarios, such as the development of population, economic indicators, land-use etc. can be found in the online at <https://tntcat.iiasa.ac.at/SspDb> based on [4].

With generation capacity given, we came up with the corresponding material use as detailed in the results of the main manuscript. To do so, we required data on the materials per unit of generation capacity for each of the 27 generation technologies in the IMAGE/TIMER energy model, which is given in Table S.2, below.

Even though the IMAGE/TIMER uses a vintage stock model based on fixed lifetimes to derive annual additions to stock (newly installed generation capacity) as described in [5], we also wanted to provide the outflow of scrap materials from electricity generation technologies, so we decided to apply a dynamic stock model, as part of an open source software platform developed & described by [6], to derive both the inflow and outflow of materials. The lifetimes are derived from [5], and are applied in combination with a standard-deviation of 0.214 times the mean lifetime, based on [7]. This translates to a relatively low spread in the lifetime distribution, which is typical for industrial capital as it is subject to standard maintenance & decommissioning contracts.

Technology	Technical lifetime (yrs)
Solar PV	25
CSP	25
Wind onshore	25
Wind offshore	25
Hydro	80
Other Renewables	30
Nuclear	60
Fossil Fuel Based	40

Table S.1. Technical lifetime assumptions for generation technologies, based on [5]. These are used in the calculation of the inflow and outflow of materials.

Technology	Concrete	Steel	Al	Pb	Glass	Based on [8]			Sources & Comments
						Cu	Co	Nd	
Solar PV		150	10.2	0.122		6.34			[9]–[12]
CSP	1351.8	576	5.50		156	3.15			[9], [12]–[14]
Wind onshore	434	121	0.87			2.73		0.02	[9], [15]–[22]
Wind offshore	509*	158	1.44			5.57		0.16	[9], [10], [18], [20], [21], [23]–[25]
Hydro	2833	71		0.005		1.70			[12], [26], [27] & 10% run-off river
Other Renewables	1026	216	3.6	0.03	31	3.90		0.04	Assumed: Average of above
Nuclear	235	43	0.08	0.034		0.76	1.2 ^{E-4}		[12], [28], table 24 & 25 in [29]
Conv. Coal	352.8	84.6	0.504			1.15	0.12		[30]–[32]
Conv. Oil	213.4	72.9	0.6			0.76	0.07		[33] or avg. of Conv. Coal/NG CC
Conv. Natural Gas	43.0	4.0	0.4			0.38	0.02		[34] or avg. of Conv. Coal/NG CC
Waste	213.4	72.9	0.6			0.76	0.07		Assumed: same as Conv. Oil
IGCC	165	34.9	0.504			1.15	0.12		[13] or if no data: same as Coal
OGCC	213.4	72.9	0.6			0.76	0.07		Assumed: same as Conv. Oil
NG CC	64.6	29	0.65			1.05	0.02		[27], [34]
Biomass CC	89.2	33.4	0.3			0.76	0.07		[13], [27]
Coal + CCS	352.8	109.2	0.504			1.63	0.12		[32], or Conv. Coal if no data
Oil/Coal + CCS	213.4	94.1	0.6			1.45	0.07		Based on 29% more steel & [32]
Natural Gas + CCS	43.0	5.2	0.4			1.07	0.03		Based on 29% more steel & [32]
Biomass + CCS	89.2	43.1	0.3			1.45	0.07		Based on 29% more steel & [32]
CHP Coal	352.8	84.6	0.5			5.59	0.12		Mn: added 10% of CHP in [35]
CHP Oil	213.4	72.9	0.6			5.21	0.07		Mn: added 10% of CHP in [35]
CHP Natural Gas	43.0	4.0	0.4			4.82	0.02		Mn: added 10% of CHP in [35]
CHP Biomass	243.8	6.2	0.05			2.94	0.07		Table 8.3 in [36]
CHP Coal + CCS	352.8	109.2	0.5			6.28	0.12		Assumed: Same as CCS variant
CHP Oil + CCS	213.4	94.1	0.6			5.90	0.07		Assumed: Same as CCS variant
CHP Nat. Gas + CCS	43.0	5.2	0.4			5.52	0.03		Assumed: Same as CCS variant
CHP Biomass + CCS	243.8	43.1	0.3			3.63	0.07		Assumed: Same as CCS variant

Table S.2. Material intensities for electricity generation technologies in ton/MW peak (or kg/kW peak capacity), corresponding to the 27 generation technologies in the IMAGE/TIMER energy model [5]. * For offshore wind farms, more information was available on steel monopile base structures, we assumed that only 10% of the base structures are composed of concrete monopiles. ** assumed to be the same as an onshore windmill. Material intensities for copper, cobalt and neodymium are based on the medium estimates found in [8].

Table S.3. Projected global average material intensities of the generation capacity (in ton/MW installed capacity) for 7 materials. These are a result of combining the changes in installed capacity (from IMAGE, see Table 2a of the main text) with the material intensities by technology as provided above (Table S.2).

	2015	2050, Baseline	2050, 2-degree
Steel	65	84	101
Aluminium	0.6	1.7	2.8
Concrete	859	691	741
Glass	0.10	1.5	3.8
Cu	1.7	2.2	2.9
Nd	0.0015	0.0044	0.006
Co	0.041	0.041	0.012
Pb	0.007	0.017	0.035

2.2 Electricity Transmission, the Grid

2.2.1 Grid Lengths

Using a preprocessed version of Open Street Maps for the year 2016, available from <http://osm2shp.ru/#Data> and the power_In files, we extracted the length of the grid lines according to the IMAGE region definition detailed in Section 1 of this document. Because underground lines are typically not identified or distinguished, the resulting line lengths were interpreted as being overhead high voltage (HV) lines, given their typically prominent visibility. Unless this was counter-indicated by any of the sparse national statistics, as displayed in Table S.4 below. It shows that the OSM data provides a reasonable estimate of HV line lengths in quite a few cases. However, it also shows cases of possible overreporting (e.g. Ukraine) or underreporting (e.g. China) compared to national studies.

	Open Street Maps	National Studies			Nature Scientific Data		
Sources:	<i>Calculation by the Authors</i>	<i>globaltransmission.info, [37],[38]</i>			<i>c (Arderne et al.)</i>		
Year of data:	2016	2013-2017			2019		
	HV	HV	MV	LV	HV	MV	LV
Canada	95,100	96,500	37,500		114,000	180,700	713,800
USA	641,400	441,900	171,900		647,700	959,800	8,647,400
Mexico	48,000	51,200	52,900	749,400	49,600	171,000	1,666,600
Central America	8,900	7,600	8,166		16,700	79,800	626,700
Brazil*	94,335	67,200			232,900	370,700	3,105,800
Rest of South America	66,800				111,300	335,600	2,462,700
Northern Africa	86,700				96,300	150,800	2,012,500
Western Africa	20,700				41,100	232,500	130,800
Eastern Africa	18,900				27,200	90,800	41,300
South Africa*	54,200	15,200			57,200	89,600	58,600
Western Europe	560,300	251,200	2,857,800	4,894,000	491,500	706,000	8,871,000
Central Europe	165,100	67,100	716,100	1,072,600	175,700	291,200	2,662,900
Turkey	45,100				55,200	171,400	1,057,000
Ukraine region*	126,400	10,400			131,500	130,300	1,301,300
Central Asia	40,600				60,600	156,100	916,100
Russia Region*	322,900	69,200			388,800	631,300	2,783,600
Middle East	123,100	123,400	94,500		135,900	337,900	2,516,300
India	319,800	273,500	298,600		422,400	693,100	604,400
Korea	9,300				14,400	36,400	536,100
China	183,900	646,500			284,500	827,000	17,508,600
South Eastern Asia	22,700				68,900	237,500	2,817,800
Indonesia Region	12,100				24,100	143,500	3,324,200
Japan*	43,800	18,800			62,700	68,600	2,122,800
Oceania	57,900	26,100			73,500	73,900	651,100
Rest of South Asia	18,700	21,900	12,200		50,700	142,700	1,952,400
Rest of Southern Africa	15,200	16,400			50,900	137,700	36,300

Table S.4. Length of grid lines in several studies, in km. Data in the first column is copyrighted by OpenStreetMap (OSM) contributors and available from <https://www.openstreetmap.org>. If available, the second column gives an indication of the grid length from national studies. Similar to [39] we assume that most of the OSM coverage represents high-voltage lines (overhead + underground). Highlighted cells indicate the numbers used in this study (average of the highlighted cells per row). Data was selected (highlighted) based on the following rationale: by default, we use the average between our own calculations and the Arderne study, unless the study by Arderne et al. reported a HV line length more than 3 times the value from national statistics (indicated with an asterisk *), in that case we chose to ignore the values from Arderne (as we expected over-reporting of the HV network in these cases) and incorporate the national estimates in the average used. In

other cases where we suspected over reporting of HV lines in the OSM data (USA, Europe, India & Oceania), we used the two lowest available values. In cases where we expected under-reporting of HV line lengths (Mexico, China, Korea, Indonesia & Rest of South Asia), we chose to ignore the two highest available estimates. For National studies, voltage levels are defined as follows: LV: <1kV, MV: 1-135kV, HV: >135kV. For the study by Arderne et al. Voltage classifications deviate slightly for the Medium & High Voltages (LV: <1kV, MV: 1-75 kV, HV: >75kV), which may explain slightly higher numbers for HV transmission line lengths.

This highlights the importance of further improving the data in the lengths of transmission lines. For now, however, the data used was deemed adequate, given that we were able to check the majority of the global circuit kilometers against at least one national study. In fact, only 12.6% of the total global circuit length used in this study (Table S.4) could not be validated against national studies. This indicates that the possible underestimation or (most likely) overestimation of the data for these countries represents a small fraction of the global line length.

Once we derived the HV voltage line lengths from Table S.4, we continue by calculating the length of lower voltage transmission lines based on a static ratio between high voltage and medium voltage (MV) or low voltage (LV) according to [38] and [39] as detailed in Table S.5. It shows that national studies provided more information on the MV network than on the length of the LV network. It is difficult to determine whether this is a realistic representation, or a definition issue due to the use of different sources for example. So, this might be an area for future research.

Region	Km MV per km HV line		Km LV line per km HV line	
	National studies	Arderne et al. [39]	National Studies	Arderne et al. [39]
Canada	0.39	1.58		6.3
USA	0.39	1.48		13.4
Mexico	1.03	3.45	14.6	33.6
Central America	1.07	4.77		37.5
Rest of South America		3.02		22.1
Northern Africa		1.57		20.9
Western Africa		5.66		3.2
Eastern Africa		3.34		1.5
Western Europe	11.4	1.44	19.5	18.0
Central Europe	10.7	1.66	16.0	15.2
Turkey		3.10		19.1
Central Asia		2.58		15.1
Middle-East	0.77	2.49		18.5
India	1.09	1.64		1.4
South East Asia		3.45		40.9
Rest of south Asia	0.56	2.82		38.5
Rest of Southern Africa		2.70		0.7
Average	3.04	2.65	16.7	18
Average used (for other regions)	2.85		17.35	

Table S.5. Transmission line length ratios. The values indicate the length of Medium Voltage lines (MV) or Low Voltage (LV) per km of High Voltage (HV) line. If multiple values are available, we apply an average. See Table S.4 for sources and the lengths of HV lines. This table excludes regions with expected under-reporting or over-reporting as discussed with Table S.4, except when a national statistics on MV/HV or LV/HV ratio were available.

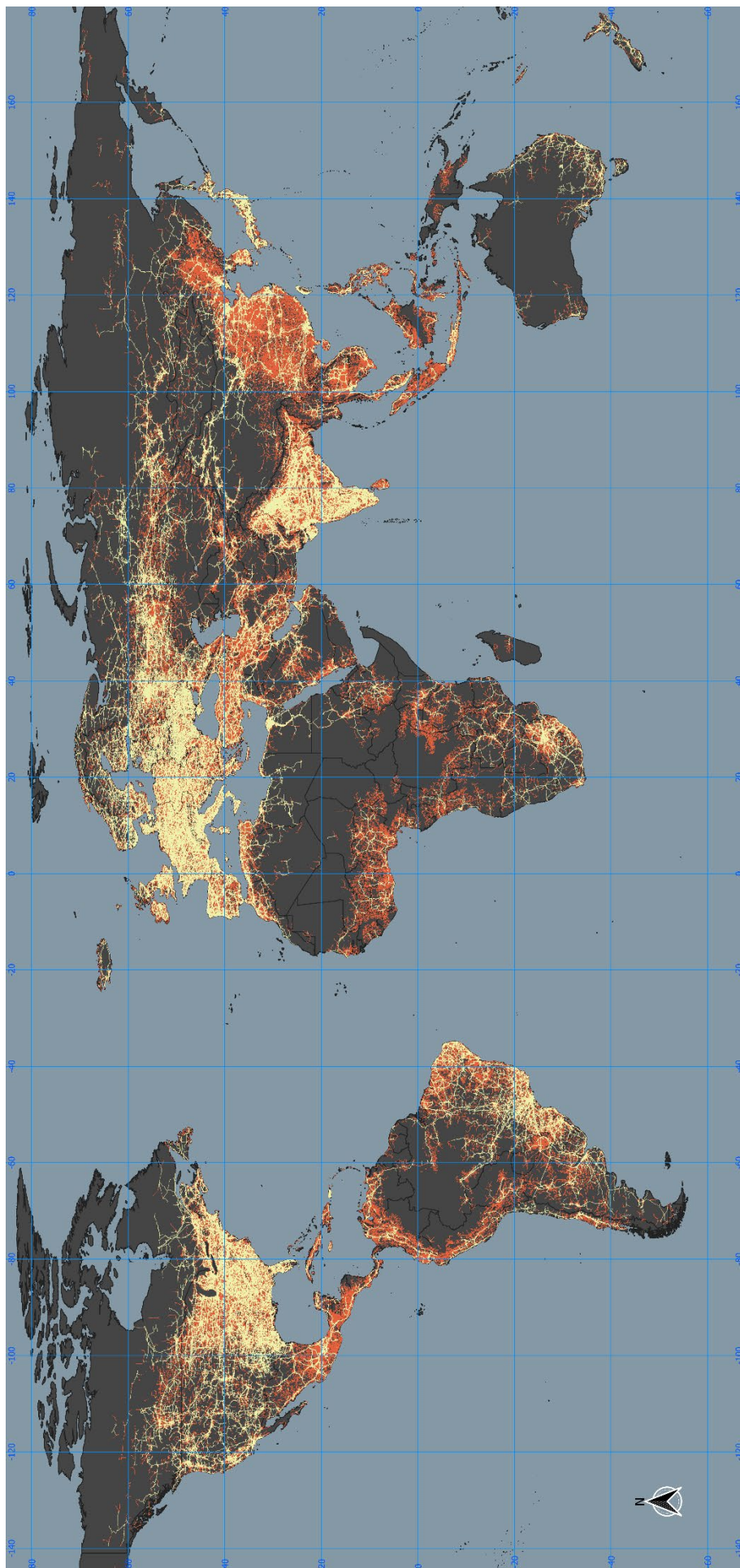


Figure S.3. Global High Voltage & Medium Voltage Transmission Lines. Data displayed here is based on the work by Arderne et al. [39], High Voltage lines are based on OpenStreetMap and displayed in yellow, Medium Voltage lines are modelled by Arderne et al. as published online at <https://gridfinder.org/>

2.2.2 Undergrounding of power lines

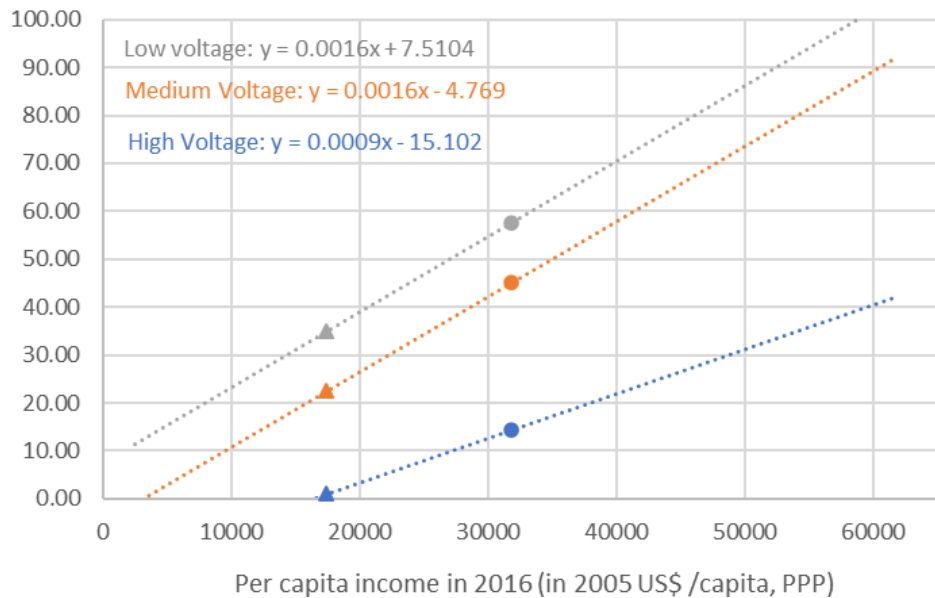


Figure S.4. Assumed relation between income levels and percentage undergrounding of transmission lines of different voltage levels, based on the indicated data points for Western Europe (circles) and Eastern Europe (triangles) as reported by [38].

2.2.3 Substations and Transformers

To incorporate additional electricity transmission infrastructure, our analysis covers the material contents of substations and transformers. To do so, we first needed to derive the demand for these elements in units per kilometer of transmission line, specified for three different voltage levels as detailed in Table S.6, below.

(units/km)	High	Medium	Low
Sources →	[40]	[40], [41]	[41]
Substations	0.0169	0.085	1.107
Transformers	0.0532	0.103	1.107

Table S.6. Assumptions on the number of substations and transformers per km of transmission line.

2.2.4 Lifetime of Grid Elements

To account for the lifetimes of power lines, substations and transformers, we applied the same dynamic stock model as described in section 2.1 of this document. We even apply the same standard-deviation, but on grid-specific mean lifetimes as detailed in Table S.7.

	Lifetime (in years)
transformers	30
lines	40
substations	40

Table S.7. Mean lifetimes applied to the grid elements. Numbers are based on [40]–[43].

2.2.5 Material Intensities of Grid Elements

Now that we have an indication of the length of the transmission line as well as the number of substation and transformers, we apply a fixed, but voltage-level specific, material intensity for each of the grid elements in Table S.8 and table S.9, below.

kg/km	Concrete	Steel	Aluminium	Cu	Pb	Glass
HV overhead	209138	52266	12883			1097
HV underground	17500			11650	14050	
MV overhead		802.3		1488		
MV underground		0	823.6	662.9		
LV overhead		0	981			
LV underground		177	531			

Table S.8. Material intensities for substations and transformers (in kg/unit). These numbers are derived using our interpretation of data from [40], [41], [43].

kg/unit	Concrete	Steel	Aluminium	Cu	Glass
Hv Substation	123900	14652	33204	4611	0.05
Mv Substation	127021	1815	1228	279.2	
Lv Substation	476	38	1228	1	
Hv Transformer	648000	296000	497	76047	
Mv Transformer	46826	22659	21	6877	
Lv Transformer	176	480	85	13	

Table S.9. Material intensities for power lines, including towers/poles (in kg/km line). These numbers were derived using the following sources: [41], [42], [44].

2.3 Electricity Storage

2.3.1 Electricity Storage Demand

Total electricity storage demand is the second main driver of the material model described in the main text and is provided as an output from the IMAGE model. Within the IMAGE model, it is calculated using a relation between the penetration of wind and solar in the mix as shown in Figure S.5. Here, we show the demand for storage capacity expressed as a fraction of the installed generation capacity as an (unweighted) average of the 8 region specific residual load duration curves (RLDCs) available from [45]. It is important to note that these RLDCs were constructed using a fixed storage price based on flow-batteries of 100\$/kWh and a round-trip efficiency of 76% [45]. This is a rather low price estimate compared to our price assumptions as detailed in Table S.13, which might mean that the assumed storage demand is on the high side.

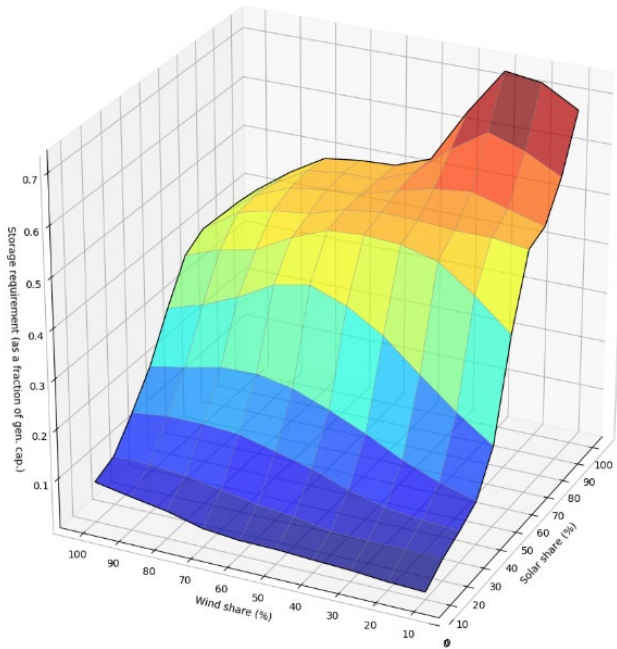


Figure S.5. Storage demand as a fraction of peak generation capacity, given different levels of solar and wind energy penetration, based on data from [45]. The numbers are an (unweighted) average of multiple regions, and only serve as an illustration of the approach to determining storage demand. Combined solar and wind shares of more than 100% are possible, because at high renewable penetration, peak demand can only be supplied by a surplus generation capacity.

2.3.2. Pumped Hydro storage

Our analysis assumes a tiered approach to electricity storage deployment, in which pumped hydro storage is the first and default option. We use projections on pumped hydro storage availability according to [46], as shown in Figure S.6.

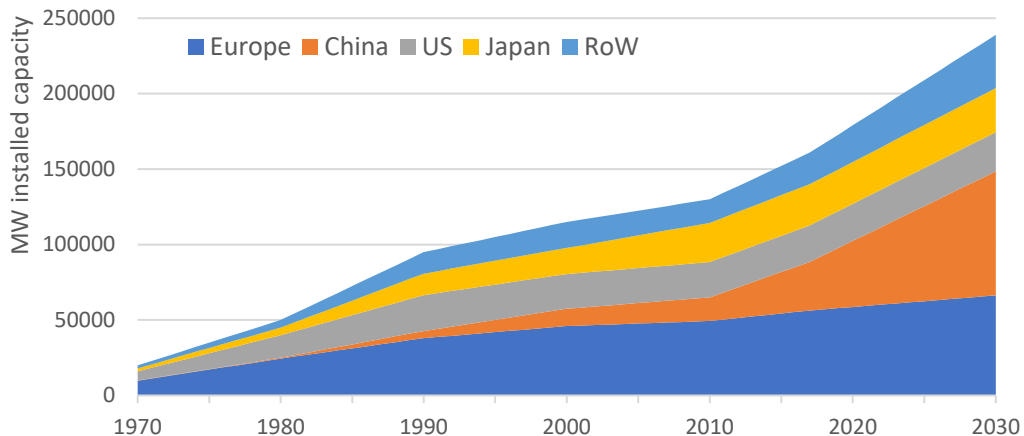


Figure S.6. Expected development of Pumped Hydro Storage availability (in MW installed capacity) according to [46]. We assume a regional disaggregation according to the IMAGE relative hydro-power capacity, and a continued growth of pumped hydro capacity according hydro-power expansion within regions [47].

2.3.3. Electricity Storage in Electric Vehicles

In order to determine the availability of electricity storage in the electric vehicle (EV) fleet we first determined the number of cars based on the IMAGE model projections described by [48] and a dynamic stock model, including lifetime assumptions, in the same way as described by [8]. Secondly, we determine the average storage capacity in current electric cars based on a review of currently available plugin- and full battery EV models according to ev-database.org, as can be seen in Table S.10.

The average battery capacity of full battery electric vehicles (BEVs) and plugin hybrid electric vehicles (PHEVs) found in Table S.10. is used to represent the recent situation and applied for the year 2018. However, battery density is expected to increase, while battery costs are expected to go down over

the coming years (see Table S.13), which could lead to a variety of possible changes to the available Vehicle to Grid (V2G) storage capacity over time. Here, we assume that the weight (and not necessarily the costs) are the limiting factor for battery deployment in EVs. This means that an increase in battery density would allow for more storage capacity, without affecting the weight of the battery unit or the car. We therefore apply a fixed battery weight, which results in a changing total battery capacity per vehicle as can be seen in Figure S.7. The figure also indicates the assumed penetration rate of vehicle to grid as a technology, which increases from 0% for 2025 (based on [49]) before reaching the maximum available percentage of the storage capacity of 10% (PHEVs) or 12% (BEVs) by 2040. Reiterating from the main text that these model settings may perhaps look optimistic regarding the adoption of vehicle to grid as a common practice, but is rooted in the idea that most of the perceived obstacles to its adoption (such as ‘range anxiety’) [50] are expected to become less of a problem given the expected increase in battery capacity as indicated in Table S.13.

BEVs			PHEVs		
Brand	Model	Capacity (kWh)	Brand	Model	Capacity (kWh)
Tesla	Model3, LR, Dual	75	Porsche	Panamera Sport Tur. 4 E-hybrid	14.1
Mercedes	EQC 400 4MATIC	85	Porsche	Cayenne E-hybrid	14.1
VW	e-Golf	35.8	Land Rover	Rover Sport p400e	12.4
Audi	e-tron 55 quattro	95	BMW	225xe iPerformance	7.6
Tesla	Model3, std range plus	55	Mitsubishi	Outlander	13.8
Kia	e-Niro	64	Mini	Countryman Cooper SE All4	7.6
MG	ZS EV	44.5	Hyundai	IONIQ	8.9
Nissan	Leaf	40			
Nissan	Leaf e+	62			
Tesla	Model3, LR, Perform.	75			
Hyundai	IONIQ	38.3			
BMW	i3 120Ah	42.2			
Jaguar	I-Pace	90			
Renault	Zoe ZE50 R110	55			
Hyundai	Kona	67.1			
Tesla	Model S	100			
Opel	Ampera-e	60			
Renault	Zoe ZE50 R135	55			
Tesla	Model X, LR	100			
Tesla	Model S, Perform.	100			
Nissan	e-NV200 Evalia	40			
Citroen	C-Zero	16			
BMW	i3s 120Ah	42.2			
Renault	Kangoo Maxi ZE33	33			
Peugeot	iOn	16			
Tesla	Model X, Perform.	100			
Peugeot	Partner Tepee	22.5			
Average		59.6	Average		11.2

Table S.10. Battery capacity of recent BEV and PHEV car models, according to ev-database.org (accessed 11-11-2019). The average from all models is used to represent the current battery capacity in our analysis.

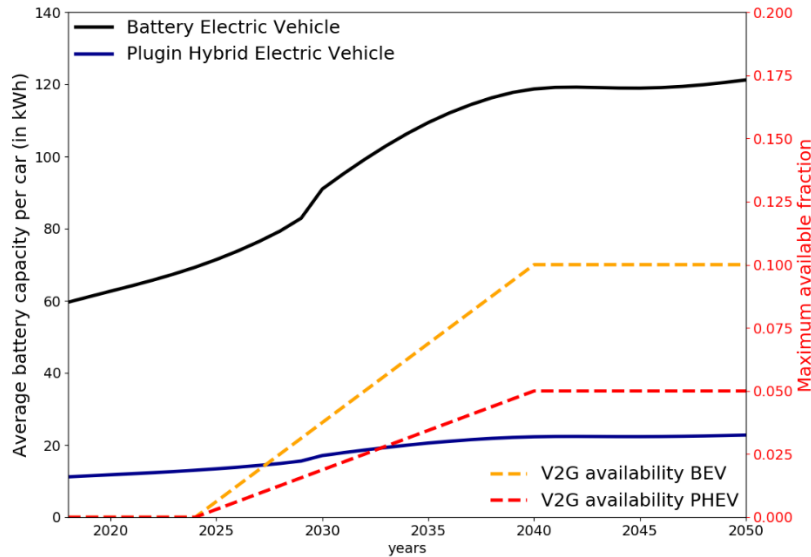


Figure S.7. development of EV & PHEV storage capacity (kWh), given a fixed battery weight assumption. Due to increased energy density of EVs, the average battery capacity will double from about 60 kWh to 120 kWh by 2040. The secondary axis displays the slow adoption of vehicle-to-grid technology from 2025 onward, ensuring a maximum of 12% of the vehicles battery capacity is available for energy storage.

2.3.4. Dedicated storage demand

Dedicated storage demand is the result of the tiered approach of the regional availability of pumped-hydro storage and electric vehicles for vehicle-to-grid storage as described in the main text. The sensitivity to regional circumstances is depicted in Figure S.8. Which shows that in many regions there is no demand for additional storage capacity, even in the SSP2 2-degree climate policy scenario, because the growth of pumped hydro and electric vehicle availability is enough to fulfill the total storage demand. Only in the regions labeled as ‘Rest of the World’ a dedicated storage capacity is required. The resulting regional deployment of dedicated storage capacity is detailed in Figure S.9.

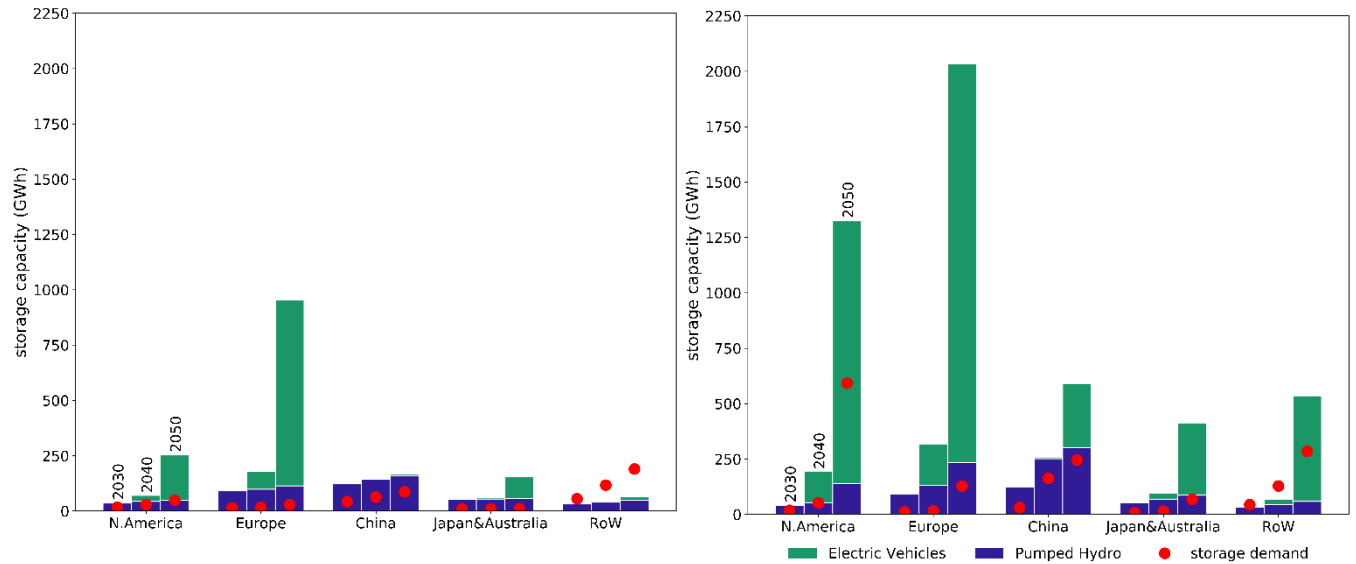
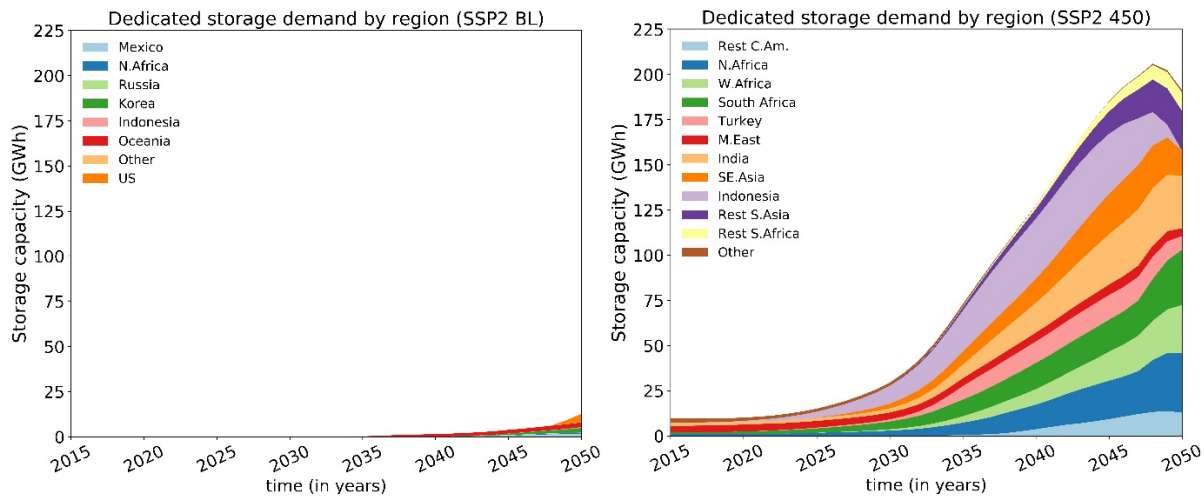


Figure S.8. Demand & supply of electricity storage capacity in 2030, 2040 and 2050, in 5 world regions, under the SSP2 Baseline (left) and under a climate policy scenario (SSP2 2-degrees, right). RoW: Rest of the World.

Figure S.9. Total demand for dedicated storage, by region. Results are given for the SSP2 baseline (left) and the SSP2, 2-degrees climate policy scenario (right).



2.3.5. Market Shares of storage technologies

Once the size of the ‘dedicated’ storage demand has been determined as the remainder of the total storage demand minus the available capacity in pumped hydro and EVs, we need to determine the market share of individual technologies to fulfill the last tier of storage. This is done based on the basis of the lowest costs per kWh (cycled, not capacity) using a multinomial logit model, as detailed in the main text. Calibration of the logit parameter uses cost data from Table S.13 and is checked against data by the IEA for the year 2016 [51] (p. 63), leading to a logit parameter (λ) setting of 0.2. A further set of cost penalties was applied to enhance the fit with the available literature by the IEA, as shown in Figure S.10. These penalties are reduced towards 2030, but the implied cost-reduction of lithium- and nickel-based batteries is maintained beyond 2030 (due to an expected second hand market for batteries from former EVs as stationary storage). The combination of a low logit parameter and the need for high cost penalties (e.g. high for Compressed Air) needed to match historic markets suggest that the energy storage sector does currently not deploy technologies according to the cost-optimality principle.

	2018	2030
Flywheel	1.5	1
Compressed Air	18	1
NiMH	0.6	0.4
LMO	0.5	0.4
NMC	0.5	0.4
NCA	0.5	0.4
Zinc-Bromide	3	1
Vanadium Redox	3	1
Sodium-Sulfur	1.5	1
ZEBRA	1.5	1

Table S.11. Cost penalties (multipliers) applied to the costs of some energy storage technologies. These multipliers are applied to the costs in Table S.13 in order to ensure a reasonable representation of the current market.

The development of the market shares over time, of both the newly installed storage capacity as well as the resulting development of the technology shares within the stock are given in Figure S.11a &b, below. The share of the stocks is based on two additional model assumptions, being: 1) that all dedicated electricity storage pre-1990 is based on deep cycle Lead-Acid batteries, and 2) a changing lifetime assumption by technology as detailed in Table S.12.

Figure S.10. Current market fit of our model compared to IEA 2017 [51].

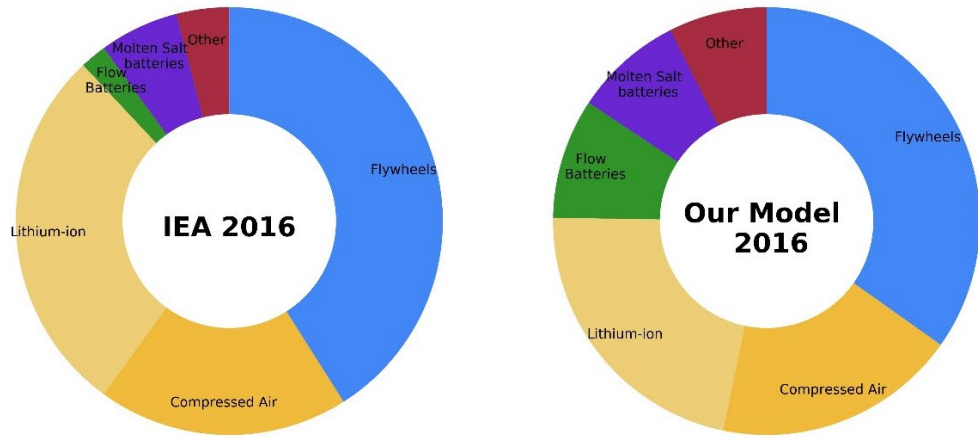
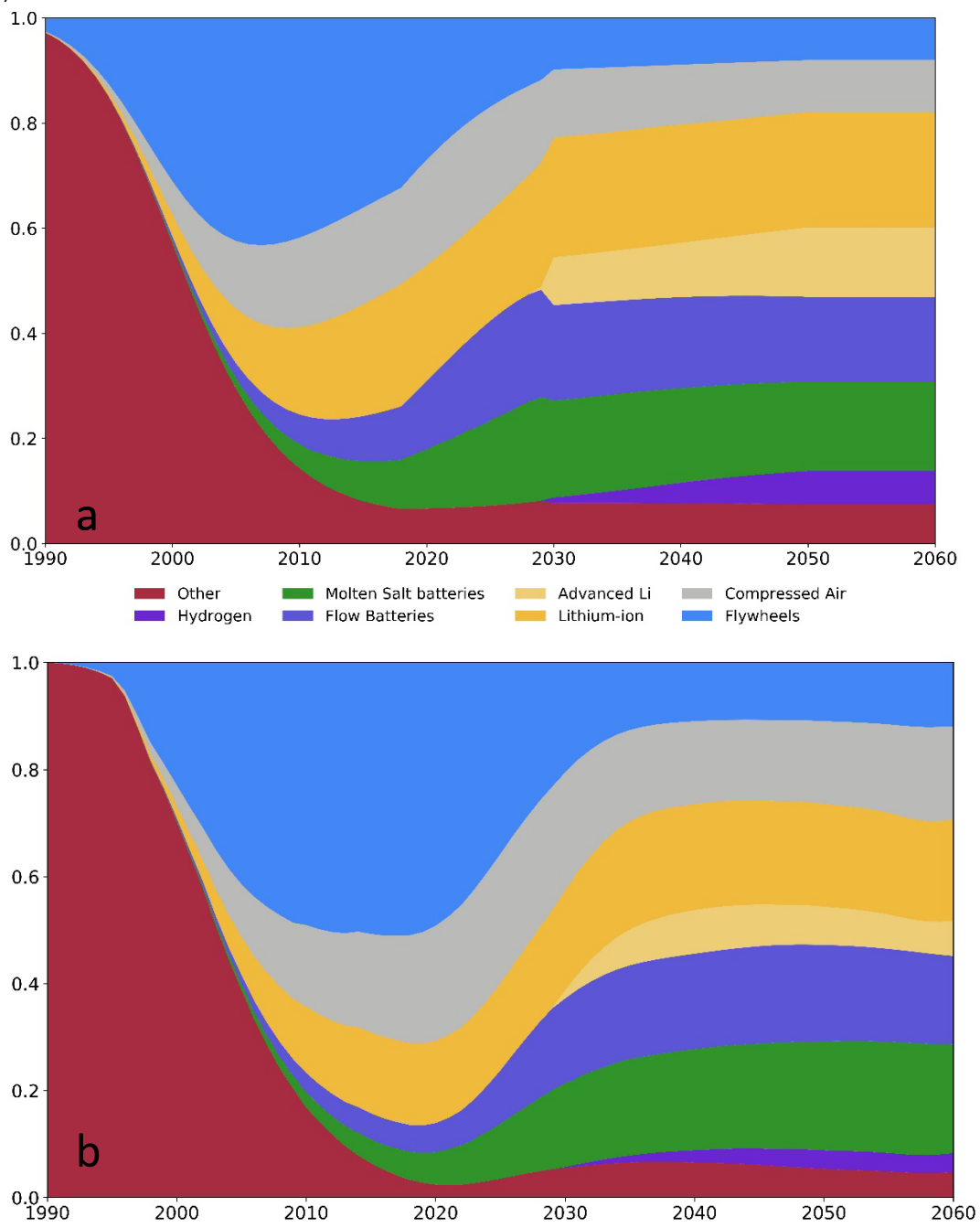


Table S.12. Lifetime assumptions for storage technologies used in dedicated electricity storage (in yrs). The lifetime is based on 150% of the indicated cycle life given in Table S.13, assuming a diurnal use or the shelf-life in years given by [52] (whichever comes first). The cycle life is extended by 50% to represent the idea that dedicated energy storage is subject to enormous capital investments and the fact that the cycle life is determined using the technical lifetime, beyond which about 80% of the storage capacity remains usable.

	Lifetime (yrs)	
	2018	2030
Flywheel	20	30
Compressed Air	50	50
Hydrogen FC	4.1	9.6
NiMH	4.1	6.2
Deep-cycle Lead-Acid	6.2	12.3
LMO	2.1	3.3
NMC	6.2	8.2
NCA	2.1	3.3
LFP	10.3	20
LTO	15	23
Zinc-Bromide	12	20
Vanadium Redox	10	17
Sodium-Sulfur	17.0	22.0
ZEBRA	15.0	22.0
Lithium Sulfur	2.15	4.11
Lithium Ceramic	2.00	10.00
Lithium-air	2.98	4.44
PHS	60	60

Figure S.11. Market shares of the dedicated electricity storage technologies (a) & shares of the technologies within the stock (b).



Now that the share of the dedicated electricity storage technologies (both stock & purchases) is known, they can be multiplied with the weights (using energy densities in Table S.13) and the weight composition as shown in Table S.14

	Technology ↓	Energy density		(dis)charge cycles		Investment costs		Round trip efficiency		
	Unit →	Wh/kg		Nr. of cycles before end of life (@80% cap.)		USD/kWh (storage capacity)		%		
Grouping	Time →	2018	2030	2018	2030	2018	2030	2018	2030	Sources
Batteries	Nickel	NiMH	75	100	1000	1500	300	300	70%	80%
	Lead-acid	Deep-cycle Lead-Acid	40	40	150	150	150	150	70%	80%
	Li-ion	LMO	121	160*	500	800	400	225	96%	98%
		NMC	185	283*	1500	2000	420	225	96%	98%
		NCA	230	300*	500	800	350	200	96%	98%
		LFP	120	212*	2500	5000	580	230	94%	96%
		LTO	65	211	7500	20000	800*	400*	98%	99%
		Flow	Zinc-Bromide	40	67	10000	10000	538	250	70%
			Vanadium Redox	25	35	15000	15000	475	131	70%
	Molten-salt	Sodium-Sulfur	200	250	6000	8000	463	145	80%	85%
		ZEBRA	186	300	4500	7500	525	110	84%	87%
	Lithium-metal (/advanced Li)	Lithium Sulfur	328	750	523	1000	375	250	91%	98%
		Lithium Ceramic	299	740	600	6000	800*	110	70%	90%*
		Lithium-air	200	250	725	1080	700	275	50%	85%
Other	Mechanical	Pumped-Hydro	1	1	50000	50000	63	63	80%	80%
		Flywheel	100	100	112500	140000	4500	2000	85%	88%
		Compressed-Air	4	5	30000	40000	86	45	52%	63%
	Fuel-cells	Hydrogen FC	157	157	1000	2333*	747	133	25%	45%

Table S.13. Cost and performance indicators for electricity storage technologies between 2018 and 2030, based on various sources. * Some values indicated with an asterisk include estimates by the authors. Only highlighted battery types are assumed to be available for mobile applications such as electric vehicles.

Grouping		Technology	Steel	Al	Plastics	Glass	Cu	Co	Ni	Pb	Mn	Nd	Sources & comments
Batteries	Nickel	NiMH	10%	0.26%	21%		1.77%	0.26%	44.3%		0.26%	4.7%	[53]
	Lead-acid	Deep-cycle Pb-Acid			10%	2%				61%			[35]
	Li-ion	LMO	21.5%	3.7%	8.4%		10 %				16.7%		[76]
		NMC	21.5%	3.7%	8.4%		10%	7.6%	7.6%		7.1%		[76]
		NCA	0.7%	24.4%			12.5%	3.1%	9.4%		2.9%		[77]
		LFP	14.1%	5%	10%*		5%						[78]
		LTO	4.5%*	14%	6.2%						7.7%		[79] and assuming: same wt% of anode as in LFP & Pure LTO as in [80]
	Flow	Zinc-Bromide	15%		4.3%		1%						[61]
		Vanadium Redox	10.6%		4.3%		0.8%						[61]
	Molten-salt	Sodium-Sulfur	30.4%		2.2%		3.5%						[81]
		ZEBRA	30.4%	11.1%	2.2%		3.5%		17.6%				[60]
	Lithium-metal (/advanced Li)	Lithium Sulfur	0.53%	18.4%	4.1%		7.82%						[65]
		Lithium Ceramic	0.53%	18.4%	4.1%		7.82%		16.8%		1.96%		Assumed: same as Li-S, but with NMC811 as cathode & wt% acc. to [79]
		Lithium-air			30.6%		9.4%						[70]
Other	Mechanical	Pumped-Hydro	94.8%	0.32%			2.17%		1.94%				Additional materials comp. to a hydro dam (Table S.2) based on [82]
		Flywheel	60.9%	20.2%			1.36%				0.64%		[83] and own calculations based on: [84], [85] and [86]
		Compressed-Air	98.4%	0.77%			0.8%						[35], [83]
	Fuel-cells	Hydrogen FC	96.2%	0.47%			1.77%						Table 34 in [35]

Table S.14. Weight composition (as a % of the total weight) of electricity storage technologies. Values indicated with an * were derived using assumptions by the authors.

3. Comparison to other sectors

In order to get a feeling for the importance of the electricity sector compared to other material demand sectors, such as buildings, we compare the growth rates of these sectors in Figure S.12. It shows that the rate of expansion of infrastructure in the electricity sector towards 2050 is larger than the growth in housing stock, and comparable to the rate of growth in commercial buildings.

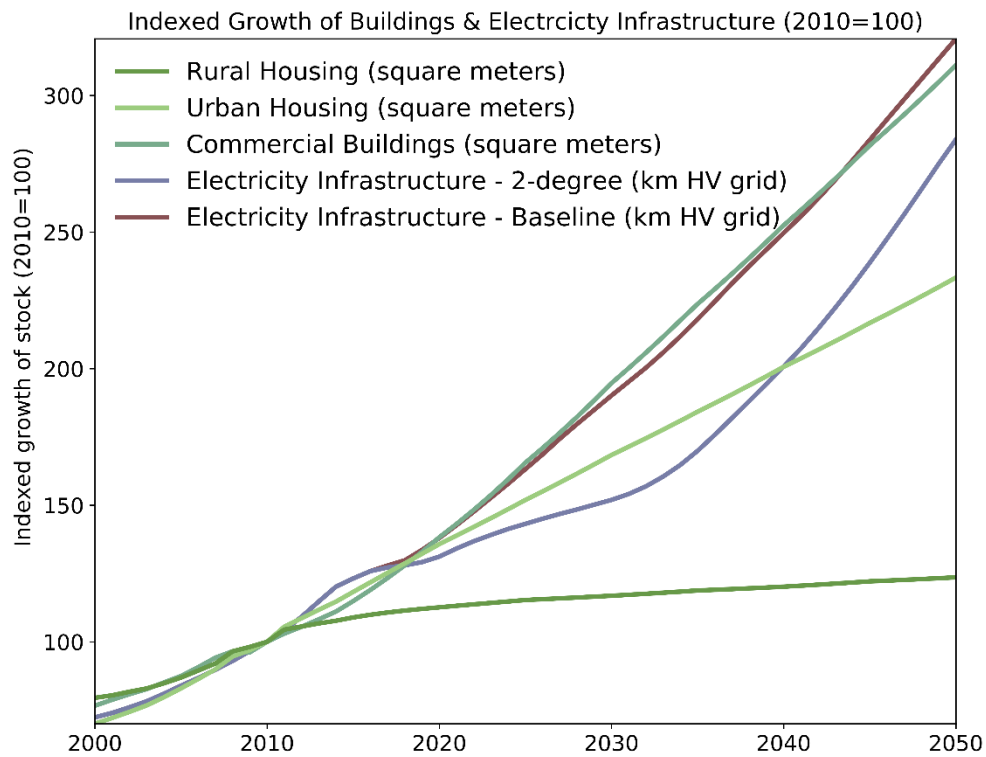


Figure. S.12. Indexed growth of Buildings and Electricity related infrastructure (2010=100). The indicators are based on the total kilometers of high-voltage (HV) grid lines discussed in this study, the development of floorspace in buildings is based on [87].

4. Sensitivity Analysis

In order to better understand the uncertainties regarding some of the assumptions and their impact on the outcomes of the presented model, we perform a sensitivity analysis. In addition to the default model outcomes presented in the main text, we define three alternative model setting to represent a range of possible future developments with relevance to the material use in the electricity sector. We focus on three key uncertainties, being 1) the development & deployment of electricity storage, 2) the extent to which the transmission infrastructure requires expansion, and 3) the uncertainty regarding future material composition of several technologies. We start by explaining the alternative model settings on transmission and storage in conjunction.

4.1 Alternative assumptions on drivers: transmission and storage

It is often highlighted that high shares of variable renewable energy such as solar and wind pose a challenge to reliably provide electricity to consumers, due to their intermittent nature [88], [89]. Backup generation capacity, energy storage technologies, grid expansion and load-shifting practices are typically proposed as options to stabilize the grid, because they may all help to alleviate the temporary imbalance between electricity supply and demand. The difficulty with defining scenarios on future energy systems is that it remains highly uncertain to which extent these stabilizing technologies will be deployed, given that they may be used interchangeably and depending on local conditions.

To account for a wider range of possible future developments of infrastructure in the electricity sector, we define two so called sensitivity variants. The first sensitivity variant is focussed on the application of additional storage capacity and the second on additional expansion of transmission capacity. It is worth noting that most of the literature that we consulted on this topic stated that storage and grid expansion are considered to be interchangeable balancing solutions in cost-optimal models (grid expansion seems to reduce the need for storage and vice versa) [88]–[91]. This is why we define the first two sensitivity variants to be mutually exclusive.

Please mind that quantitative scenarios on global deployment of transmission infrastructure or storage capacity are scarce and the few studies that exist present a wide range of possible outcomes [88]. For example, the need for storage capacity in Europe towards 2050 could be much higher than our default model [90], but could also be negligible [92]. Therefore, we often had to define the sensitivity variants based on our own judgement and some proxys from data on Europe. We present and explore the effects on the model results only to get a better understanding of the sensitivities of the model and to identify materials for which the demand is highly dependent on the scenario storyline, and therefore more uncertain.

4.1.1 Sensitivity variant 1: high storage, low V2G, low PHS

The first sensitivity variant assumes a higher storage demand by doubling the required storage capacity towards 2050. This alternative assumption could be justified by [92], who find that the European storage requirements as reported by the IMAGE model might be low compared to other models. Combined with pessimistic assumptions on the adoption of vehicle-to-grid storage, this sensitivity variant could be considered a worst-case scenario, aimed to explore the additional material demand in dedicated (stationary) storage under less favourable conditions.

compared to the default assumptions, the regional storage capacity is doubled between 2020 and 2050, while the available storage capacity in electric vehicles is halved towards 2050. Additionally, the installed capacity of Pumped Hydro Storage (PHS) does not grow after 2030 (the end of the predictions by the IHS [46]) and 50% of the remaining regional storage demand (after PHS) is considered to be fulfilled by dedicated storage, which could be due to financial incentives for consumer which produce their own electricity (prosumers, e.g. through rooftop PV) and might benefit from investing in distributed stationary storage applications (after [89], [90]).

Implications for global storage capacity can be found in Figure S.15, and the effects on overall material use are discussed in section 4.3. Figure S.13, below, shows the implications of the ‘high storage’ assumptions on regional storage deployment towards 2050. For comparison to the default model setting, please see Figure S.9.

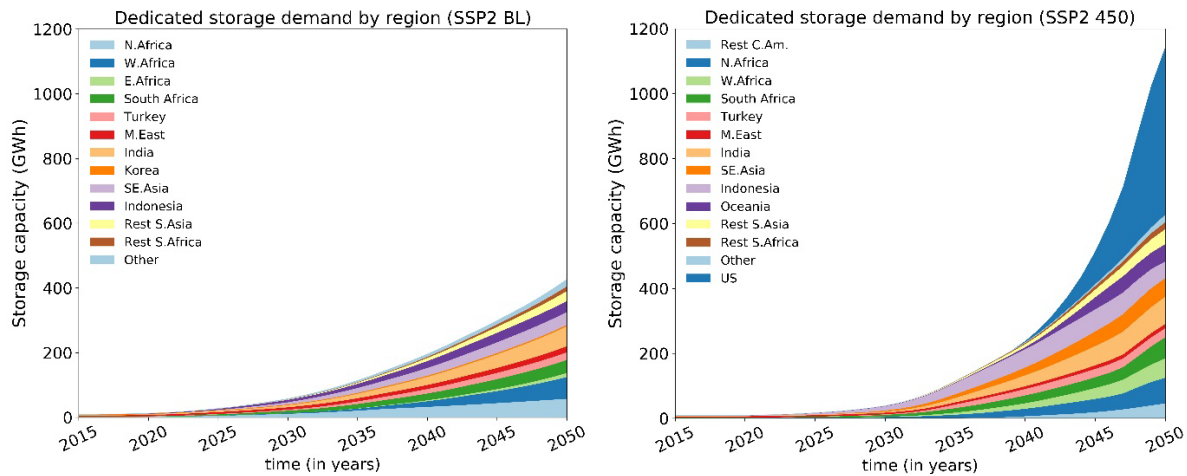


Figure S.13. Regional deployment of dedicated storage under the ‘high storage’ sensitivity variant. Results are given for the ‘high storage’ sensitivity variant of the SSP2 baseline and the ‘high storage’ sensitivity variant of the SSP2, 2-degrees climate policy scenario (right).

4.1.2 Sensitivity variant 2: high transmission expansion

Under the high transmission expansion assumptions we implement a slightly different growth of the high voltage (HV) electricity transmission network, while maintaining the default length of the Medium and Low voltage levels. We choose to do so, because most available studies only elaborate on the expansion of HV (interregional) transmission capacity, see for example [90], [93]. Based on these two studies with quantitative indications on the additional transmission line length in renewable energy scenarios for Europe (Figure S.14), we conclude that our default assumptions on the expansion of HV transmission line lengths might be on the high side in the SSP2 Baseline scenario, while in the SSP2 2-degree scenario it might be on the low side.

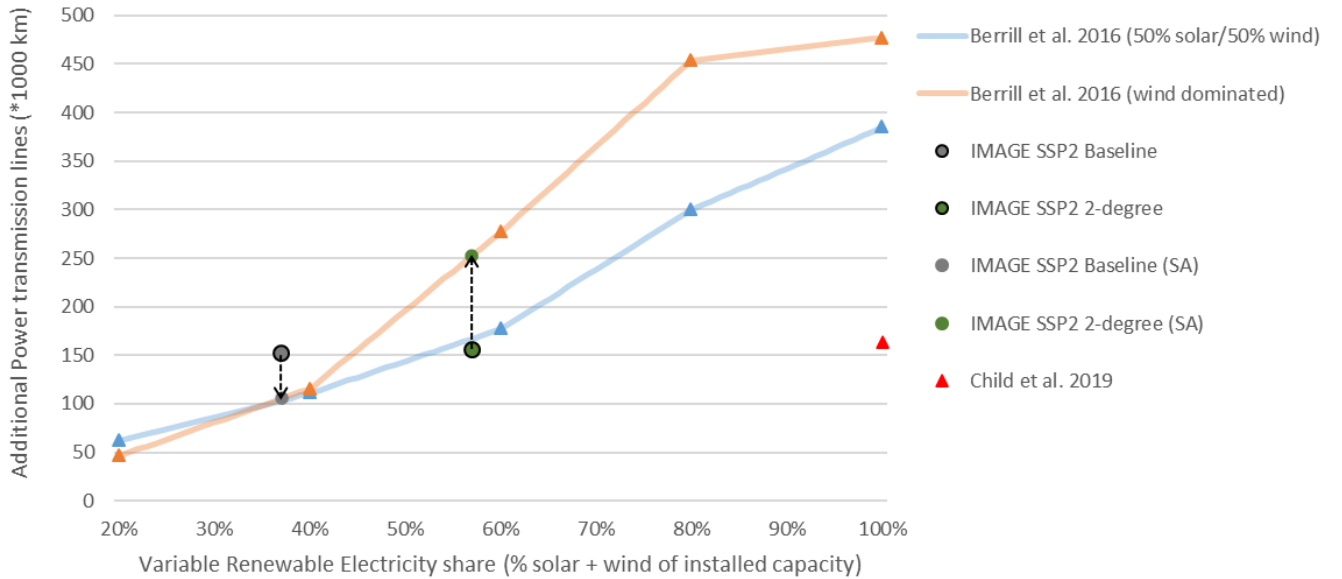


Figure S.14. European High Voltage transmission line expansion (in 1000 km) under different renewable energy shares. Shown are results from two studies compared to our own assumptions using the SSP2 scenario based on the IMAGE model baseline and the 2-degree climate policy assumptions. The arrows indicate the consequences of the sensitivity variant 2, which make the model more sensitive to the adopted levels of variable renewable electricity generation.

To explore the effects of a model with a HV line length that is a little more sensitive to the penetration levels of variable renewable energy, we adjust our growth assumptions so that variable renewable electricity generation (PV Solar & Wind) will lead to a 100% larger demand for grid expansion, while other baseload technologies require 70% less grid expansion towards 2050. As such a 100% growth of a fully fossil-based generation capacity would lead to a 30% increase in the HV line length, but a 100% growth in a fully renewable-based generation capacity would lead to a 200% increase in HV transmission line length in the end of the scenario. Though these assumptions should be verified with data on other regions, it can be seen in Figure S.14 that for Europe this would lead to an additional HV line length that seems comparable to the range found in [93].

Together, the two sensitivity variants describe an alternative development of the drivers of material demand in electricity storage and HV grid lines, as displayed at the global scale in Figure S.15.

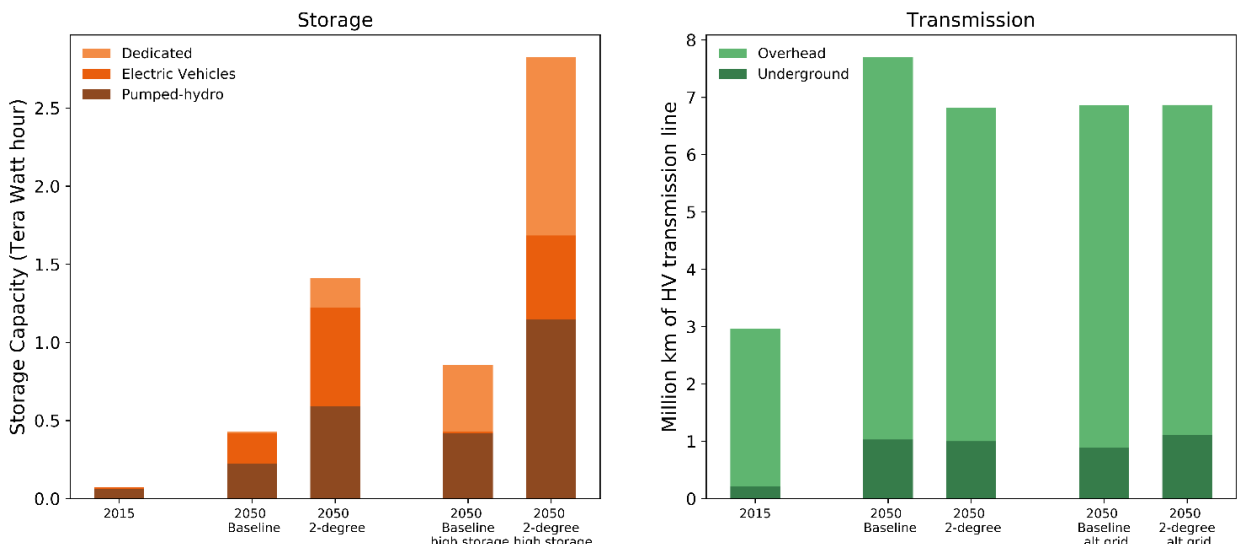


Figure S.15. Alternative assumptions on storage capacity and transmission line length under two sensitivity variants (high storage & alt. grid). These panels show the assumptions used in the sensitivity analysis. While the higher storage demand ('high storage') mostly affects the 2-degree scenario, the baseline is most affected by the alternative assumptions on grid expansion ('alt. grid'). Even though the differences between the baseline and the 2-degree scenario seem small when implementing the alternative grid settings ('alt. grid') the 2-degree scenario now has a larger HV grid, despite much lower generation capacity, which was a consequence of higher efficiency improvements under stricter climate policy assumptions in the IMAGE SSP2 scenario.

4.2 Alternative assumptions on material intensities

The use of static material intensities in our default model assumptions is not just a convenient modellers choice. There is an inherent uncertainty about technological developments into the future, which simply makes it impossible to model the expected changes in material intensity towards 2050 for all of the 28 generation technologies, the 17 storage technologies, the materials involved in the infrastructure of 6 different line types as defined in this study. Instead, we explore the impact of three foreseeable changes in the material composition of a few of the technologies used for generation, transmission and storage based on sparsely available literature . The details are discussed below, followed by an elaborate discussion on the outcomes of the sensitivity analysis based on the three different santsity variants.

4.2.1 Sensitivity variant 3: dynamic material intensities

First of all, we model the potential impacts of reduced cobalt content in lithium-ion batteries after a recent study by [94]. This sensitivity variant enforces a continually decreasing cobalt content of NCA & NMA battery types between 2020 and 2050, effectively eradicating cobalt from these battery types in new batteries by 2050. Mind that this battery composition change is enforced simultaneously with the battery density improvements that are part of the default assumptions. Given that we do not assess the demand for nickel, we are unable to fully assess the trade-off in terms of additional demand for substituting materials.

Secondly, we explore the possible impact of an increasing share of transmission lines being High Voltage Direct Current (HVDC lines) between 2020 and 2050. Though the default model does not strictly distinguish between Alternating Current (AC) or Direct Current (DC) transmission and bases the material intensities of underground cables on a mix of both AC & DC lines found in [44], the sensitivity variant addresses the possible increase in the share of new HVDC lines (especially in intercontinental transmission) [91] by increasing the copper content of underground HV lines, which is notably higher in HVDC lines [44], to represent 75% of the additions to be HVDC by 2050 (up from 50% in the default scenario). In terms of material intensity, this represents a 13% increase in the copper content (in kg/km).

Finally, we implement an annual material efficiency improvement of the structural use of steel and aluminium in solar- and wind based generation technolgies between 2020 and 2050. Given that these technolgies are still in development, we address the posibility of ongoing improvements in material efficiency of the newly installed generation capacity, by assuming an annual material efficiency improvement of 1%. Over the 2020-2050 period this would lead to a 26% decrease in the material intensity (kg/MW) for wind and solar technologies. This could for example be achieved through the development of lighter solar panels [95] or through the increased substitution of materials in windmills by composites [96] or even wood [97].

4.3. Results of the Sensitivity Analysis

Figure S.16 shows the results from the sensitivity analysis in terms of total stock for the four materials that are affected by each sensitivity variant. Table S.15 shows more details regarding the deviation from the reference scenarios (the SSP2 Baseline & 2-degree scenario) towards 2050, including the consequences on material inflow, outflow and the resulting ratio. Table S.16 shows some additional details with regard to the material use in dedicated storage applications.

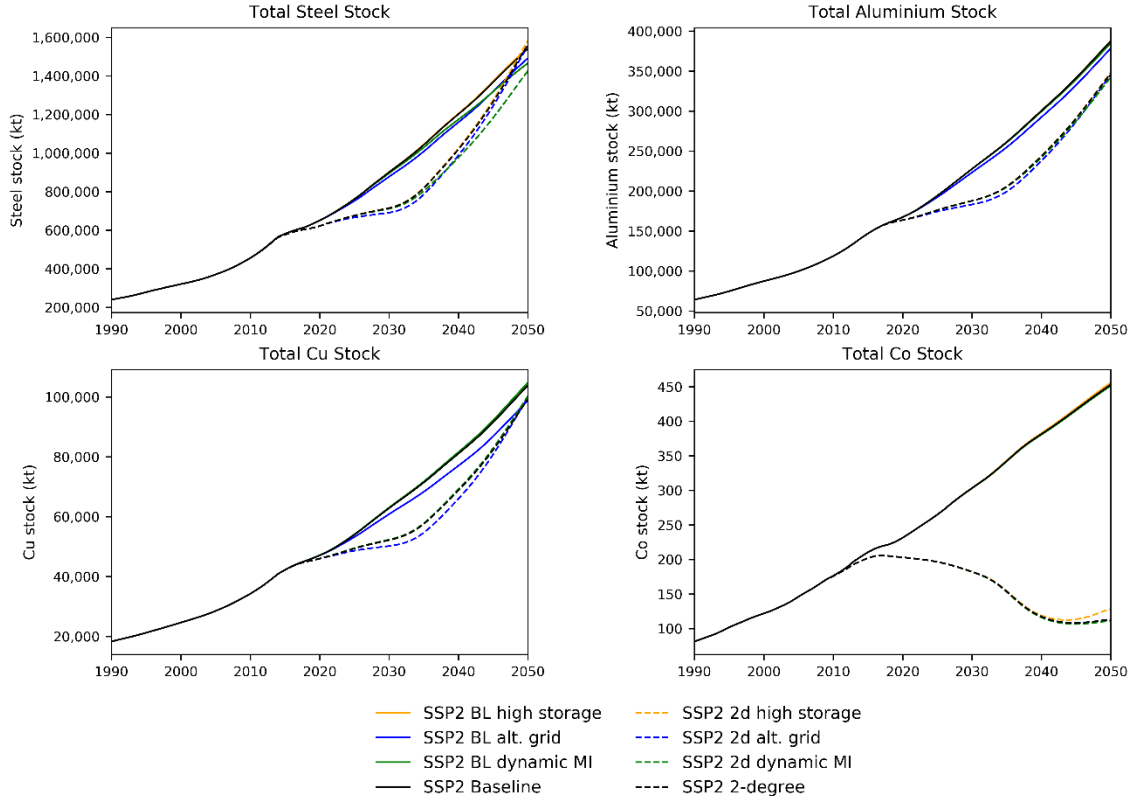


Figure S.16. Results of the sensitivity analysis on the stock of steel, aluminium, copper (Cu), and Cobalt (Co). Dashed lines describe the SSP2 2-degree scenario and its sensitivity variants. A solid line refers to the Baseline.

		Sensitivity Analysis: Difference in 2045-2050 results					
		SSP2 Baseline			SSP2 2-degree scenario		
		Alt. grid	High storage	Dynamic MI	Alt. grid	High storage	Dynamic MI
Stock	Steel	-3.4%	0.4%	-4.2%	-1.0%	1.1%	-7.7%
	Aluminium	-2.6%	0.1%	-0.6%	-0.9%	0.3%	-1.3%
	Cu	-5.0%	0.1%	0.9%	-0.5%	0.4%	0.9%
	Co		0.6%	-0.3%		9.0%	-1.5%
Inflow	Steel	-1.3%	0.7%	-8.6%	3.3%	2.3%	-12.8%
	Aluminium	-0.8%	0.2%	-1.3%	2.9%	0.9%	-2.1%
	Cu	-2.7%	0.2%	1.3%	7.6%	1.0%	1.4%
	Co		2.8%	-1.5%		60.3%	-6.4%

Table S.15. Results of the sensitivity analysis: percentage deviation of the three sensitivity variants compared to the default model outcome by the end of the scenario period (average of 2045–2050). Shown are the deviations in terms of total stock and in terms of inflow, for those materials that are affected by the three sensitivity variants, being: 1) alternative growth of the high voltage grid ('alt. grid'), 2) High storage demand combined with pessimistic assumptions on the availability of pumped hydro storage and vehicle-to-grid technology ('High storage') and 3) implementing a dynamic material intensity

based on foreseeable shifts in technologies of material efficiencies ('dynamic MI'). Readers guide: the 'dynamic material intensity' variant, which implements a 1% annual steel efficiency improvement in solar- and wind-based electricity generation, causes a 4.2% decrease in the steel contained in stocks over the last five years of the SSP2 Baseline, compared to the last five years of the default Baseline explored in the main text (e.g. Table 2).

The alternative assumptions explored in the three sensitivity variants do not have a large effect on the amount of materials contained in the stock. For the period 2045 to 2050, the largest increase compared to the default assumptions is a 9% increase in cobalt stocks under alternative storage assumptions in the 2-degree scenario. The largest decrease in material use found for the same period is 7.7% less steel as a consequence of the dynamic material intensities (due to a 1% annual material efficiency improvement in solar- and wind-based electricity generation).

The effects of the sensitivity analysis on the inflow indicators are larger. For the inflow, the largest increase related to the sensitivity variants is also found for cobalt and steel. However, the roughly 13% decrease of annual steel demand (i.e. inflow) and the roughly 60% increase in annual cobalt demand show a larger effect of the sensitivity analysis on the inflow indicators. The large increase of cobalt demand in the 'high storage' variant of the 2-degree scenario can be explained by the assumed doubling of the storage capacity, and an increase of the share of dedicated electricity storage in a period that other uses of cobalt (such as high-temperature steel in electricity generation) are no longer expanding their stock.

Based on the sensitivity responses of the 'high storage' and the 'dynamic material intensity' variants, it seems fair to conclude that the uncertainty regarding the analysis of the material use in the electricity sector seems to increase when looking at a climate policy scenario and may be even more pronounced when focusing on inflow indicators. The only case where this doesn't seem to hold is in the variant exploring 'alternative grid' expansion rules under baseline conditions, this has to do with the timing of the deployment of generation capacity and, consequentially, the lower grid size. Here, the inertia of the stock composition causes a lag between changes in the materials inflow and the materials in the stock.

The 'high storage' sensitivity variant specifically, could have large consequences on the demand for materials in dedicated storage applications, as shown in Table S.16. Compared to the default model settings, the materials contained in the in-use stocks is more than doubled. Differences between materials occur due to the dynamic deployment of different storage technologies, each with their own material composition. While in-use stocks for steel and copper grow by a factor 2.1 in the 2-degree scenario, cobalt stocks grow by a factor 5.2. This effect is higher than expected based on the doubling of total storage demand alone. Therefore, the future availability of vehicle-to-grid storage capacity (and to a lesser extent that of pumped hydro), could play an important role in lowering material demand for dedicated storage applications.

	Default settings		'high storage' sensitivity variant	
	Baseline	2-Degree	Baseline	2-Degree
	2015	2050	2050	2050
Steel	1566	6943	14400	12800
Aluminium	63	302	375	597
Glass	0.4	6.1	7.7	13
Cu	35	161	334	300
Nd	1.8	8.3	10	17
Co	0.1	1.9	2.4	4.4
Pb	11.7	98	126	217
				537

Table S.16. In-use material stocks for dedicated electricity storage under the 'high storage' sensitivity variant by 2050 (in kt). Similar to Table S.15, results are shown for the SSP2 baseline and the SSP2 2-degree scenario and values refer to an average of model outcomes (2010-2015 & 2045-2050).

5. Model Code

The python code used for the analysis is made available for review and future improvement online, via github.com/SPDeetman/ELMA

This repository also contains the raw output data used in the plots of the detailed results in the following section. In case of future improvements or corrections, updates will be posted and managed there.

6. Detailed results

a. Steel

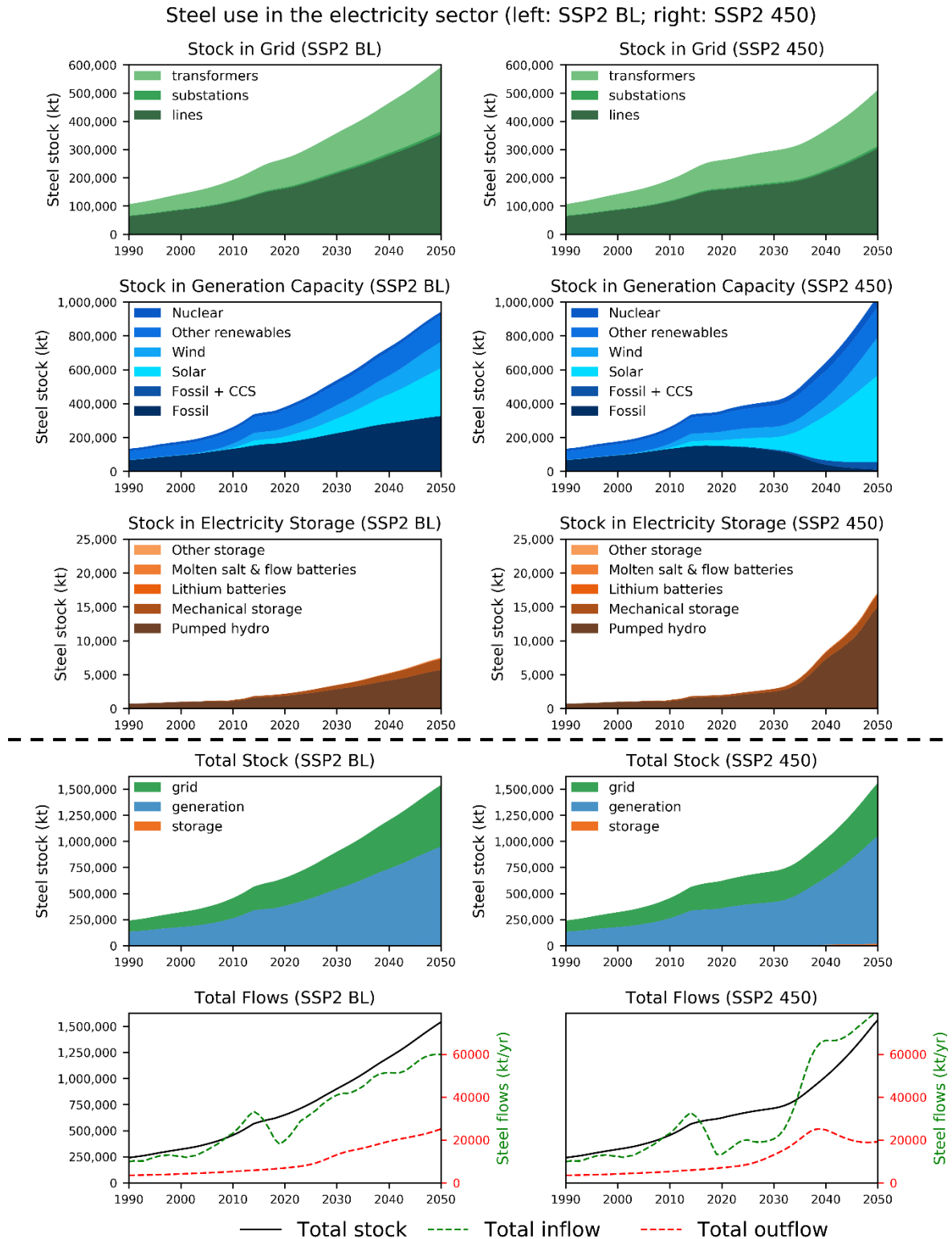


Figure S.17. Steel use (stocks & flows) in the electricity sector. The upper 6 graphs show the stocks in generation, transmission and storage technologies, while the lower 4 graphs show the total stock and flows.

b. Aluminium

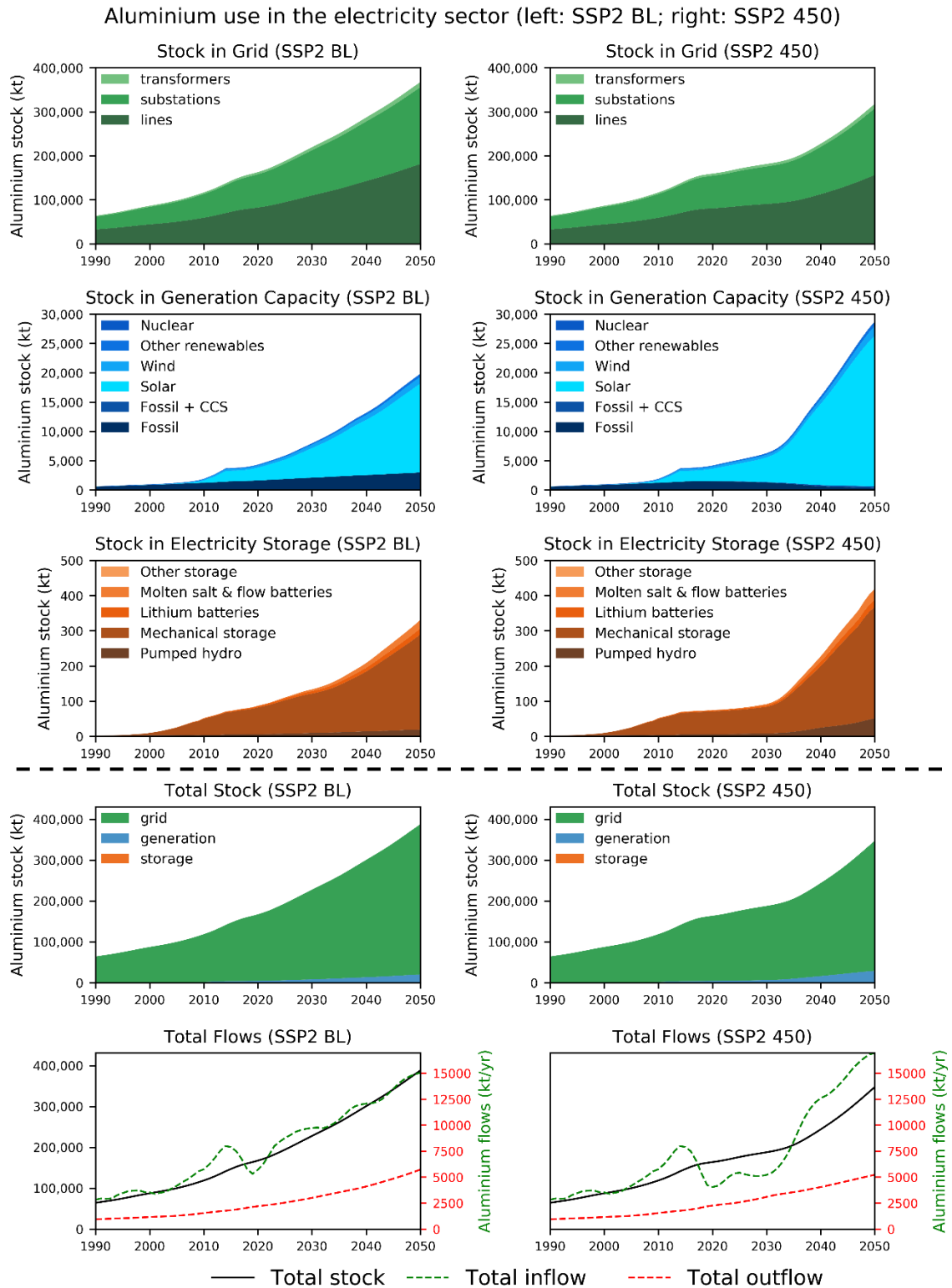


Figure S.18. Aluminium use (stocks & flows) in the electricity sector. The upper 6 graphs show the stocks in generation, transmission and storage technologies, while the lower 4 graphs show the total stock and flows.

c. Concrete

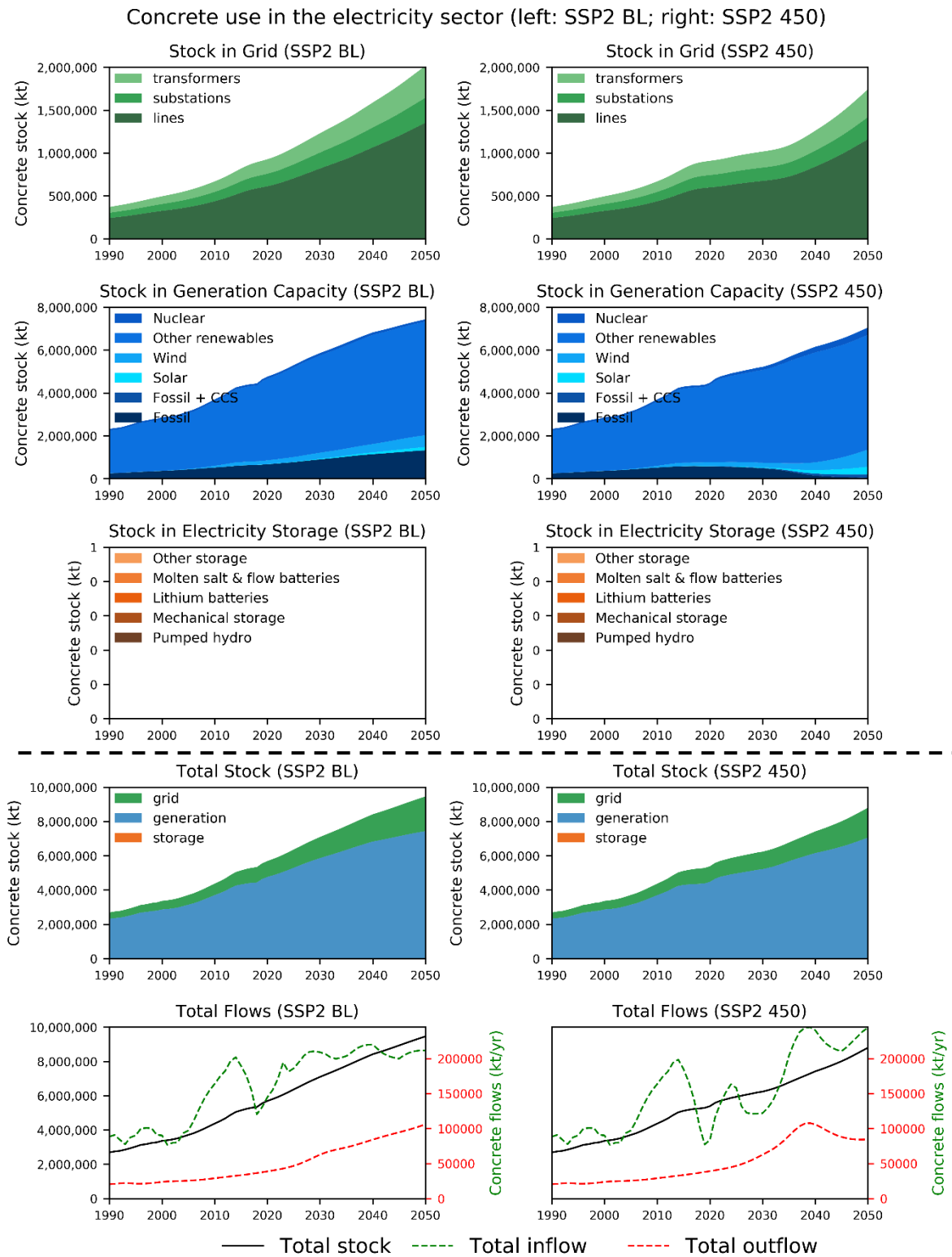


Figure S.19. Concrete use (stocks & flows) in the electricity sector. The upper 6 graphs show the stocks in generation, transmission and storage technologies, while the lower 4 graphs show the total stock and flows.

d. Glass

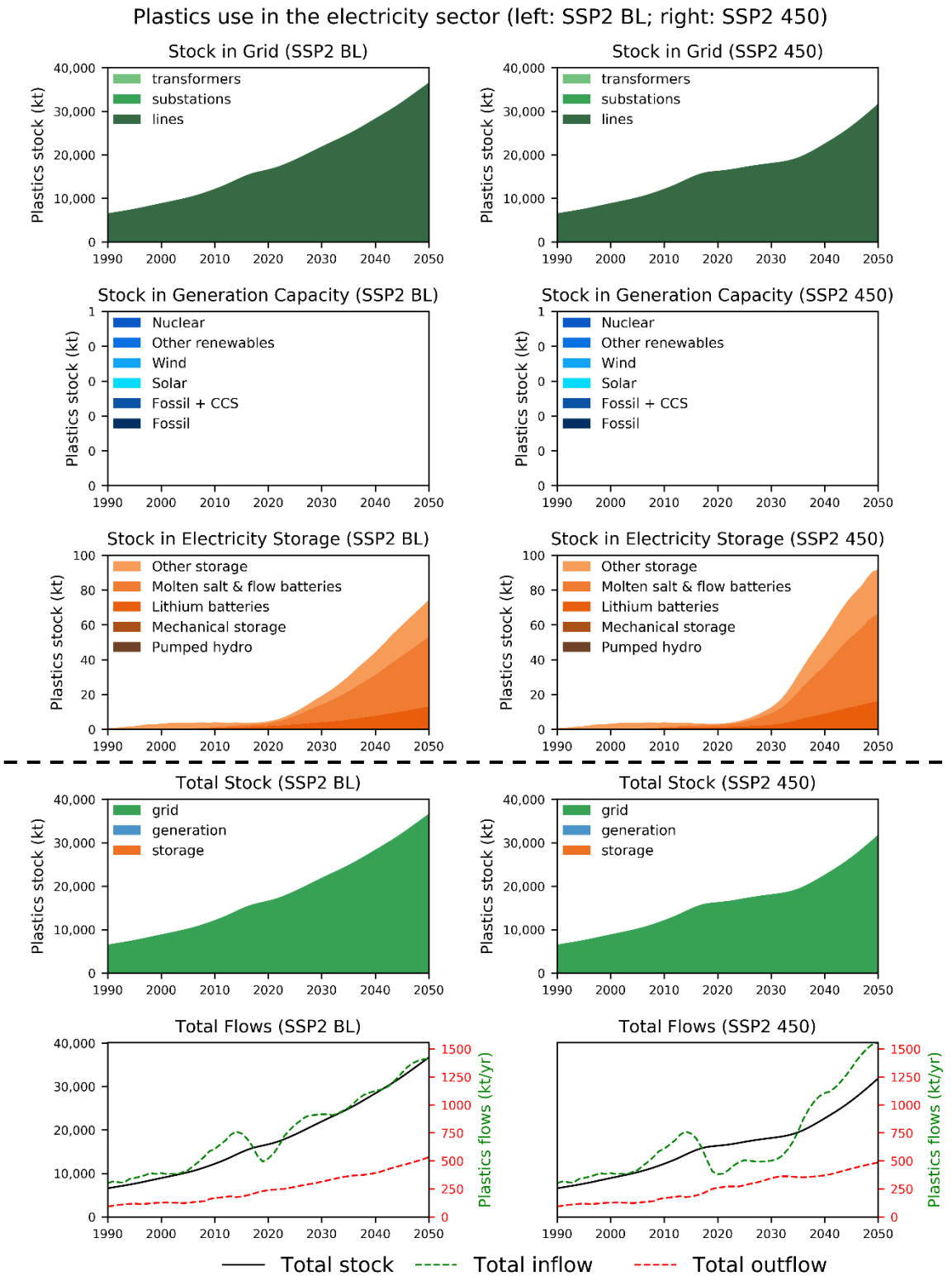


Figure S.20. Glass use (stocks & flows) in the electricity sector. The upper 6 graphs show the stocks in generation, transmission and storage technologies, while the lower 4 graphs show the total stock and flows.

e. Copper

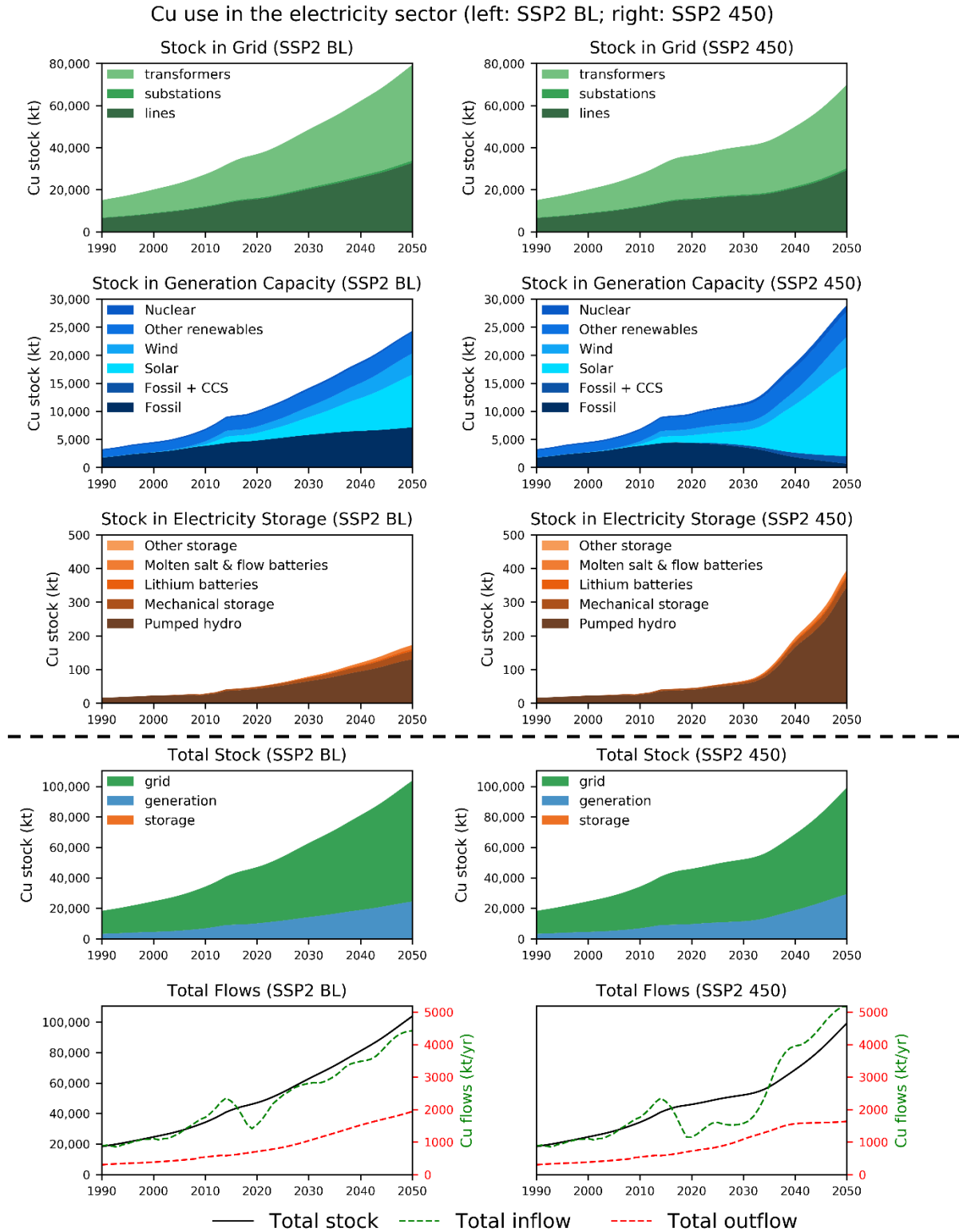


Figure S.21. Copper use (stocks & flows) in the electricity sector. The upper 6 graphs show the stocks in generation, transmission and storage technologies, while the lower 4 graphs show the total stock and flows.

f. Neodymium

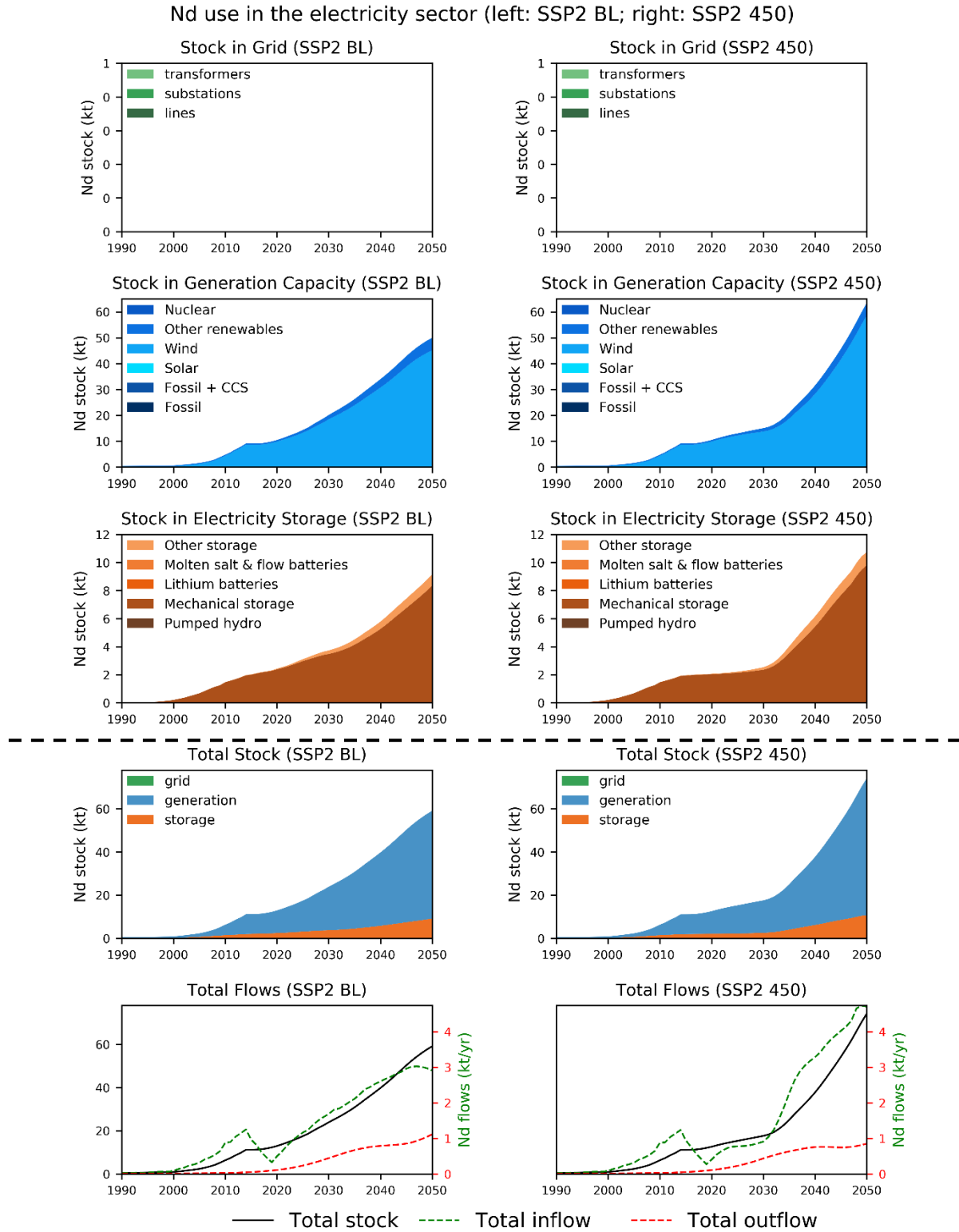


Figure S.22. Neodymium use (stocks & flows) in the electricity sector. The upper 6 graphs show the stocks in generation, transmission and storage technologies, while the lower 4 graphs show the total stock and flows.

g. Cobalt

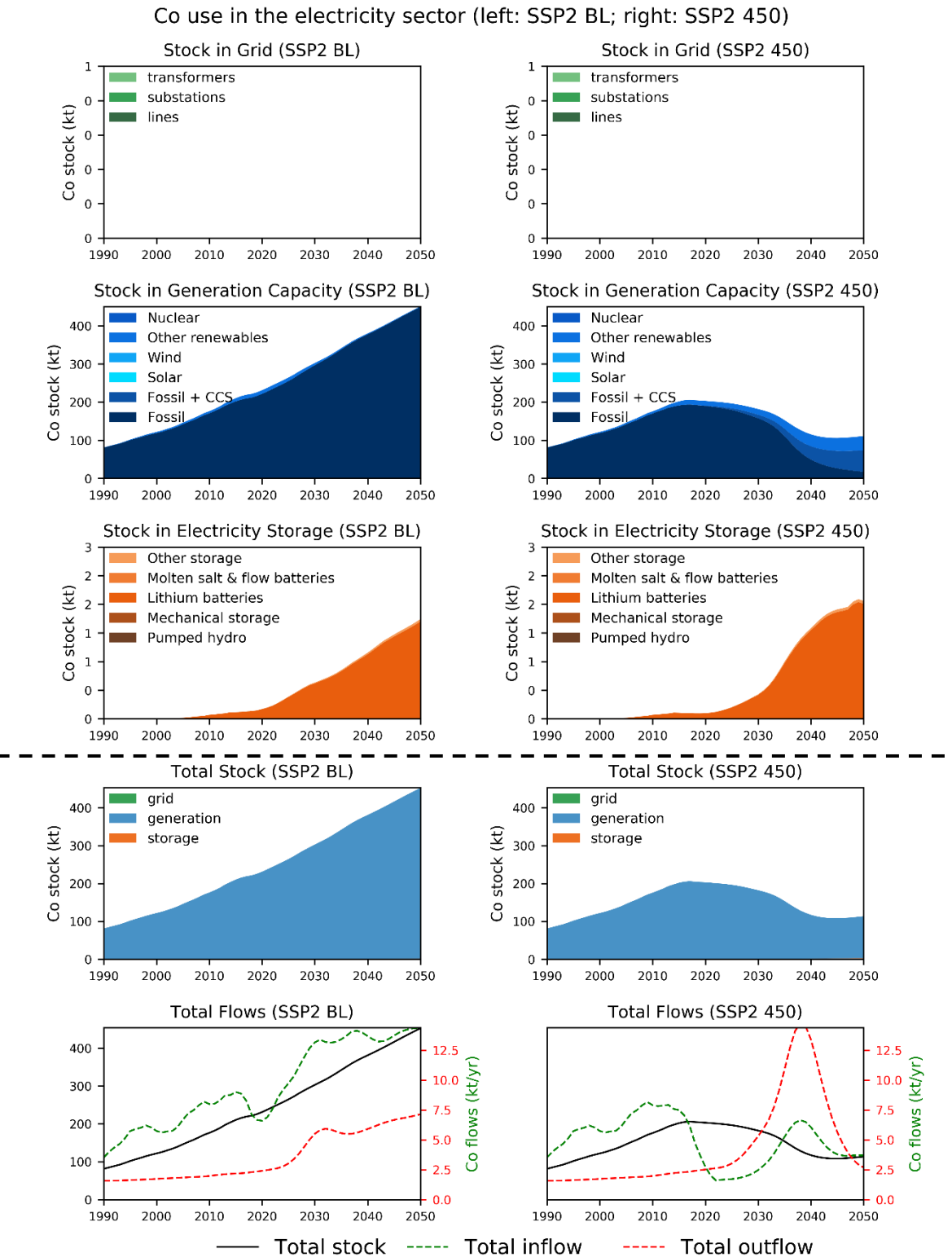


Figure S.23. Cobalt use (stocks & flows) in the electricity sector. The upper 6 graphs show the stocks in generation, transmission and storage technologies, while the lower 4 graphs show the total stock and flows.

h. Lead

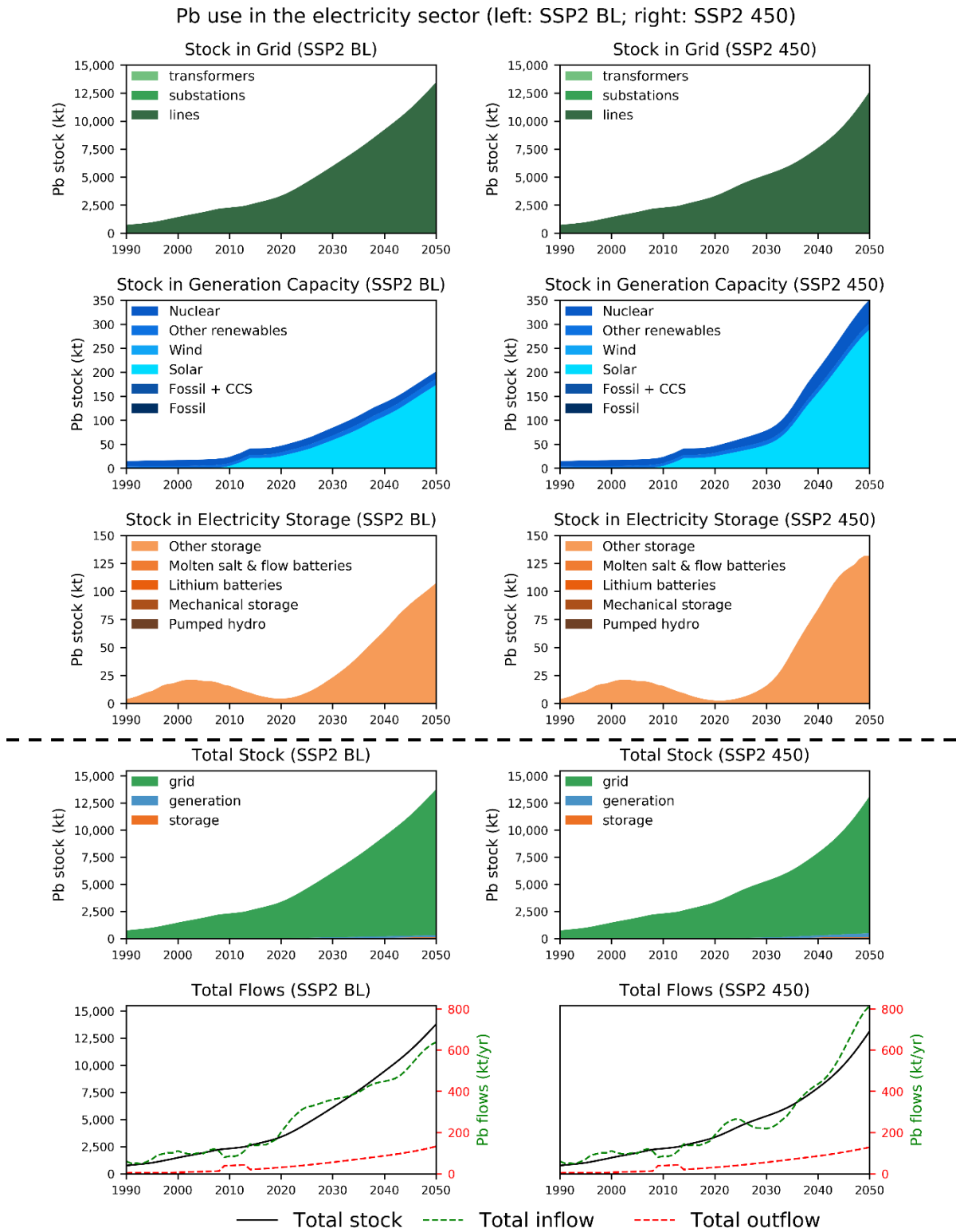


Figure S.24. Lead use (stocks & flows) in the electricity sector. The upper 6 graphs show the stocks in generation, transmission and storage technologies, while the lower 4 graphs show the total stock and flows.

References to the Supplementary Information

- [1] E. Stehfest, D. van Vuuren, L. Bouwman, and T. Kram, *Integrated assessment of global environmental change with IMAGE 3.0: Model description and policy applications*. Netherlands Environmental Assessment Agency (PBL), 2014.
- [2] E. Stehfest, D. van Vuuren, T. Kram, and L. Bouwma, *Integrated Assessment of Global Environmental Change with IMAGE 3.0*. The Hague, the Netherlands: PBL Netherlands Environmental Assessment Agency, 2014.
- [3] D. P. van Vuuren *et al.*, “Energy, land-use and greenhouse gas emissions trajectories under a green growth paradigm,” *Glob. Environ. Chang.*, vol. 42, pp. 237–250, 2017.
- [4] K. Riahi *et al.*, “The Shared Socioeconomic Pathways and their energy, land use, and greenhouse gas emissions implications: An overview,” *Glob. Environ. Chang.*, vol. 42, pp. 153–168, Jan. 2017.
- [5] D. P. van Vuuren, “Energy systems and climate policy - Long-term scenarios for an uncertain future,” Utrecht University, 2006.
- [6] S. Pauliuk and N. Heeren, “ODYM—An open software framework for studying dynamic material systems: Principles, implementation, and data structures,” *J. Ind. Ecol.*, p. jiec.12952, Oct. 2019.
- [7] G. Balzer and C. Schorn, *Asset Management for Infrastructure Systems: Energy and Water*. Springer International Publishing, 2015.
- [8] S. Deetman, S. Pauliuk, D. P. van Vuuren, E. van der Voet, and A. Tukker, “Scenarios for Demand Growth of Metals in Electricity Generation Technologies, Cars, and Electronic Appliances,” *Environ. Sci. Technol.*, vol. 0, no. 0, p. null, 2018.
- [9] A. Elshkaki and T. E. Graedel, “Dynamic analysis of the global metals flows and stocks in electricity generation technologies,” *J. Clean. Prod.*, vol. 59, pp. 260–273, 2013.
- [10] I. Öhrlund, “Future Metal Demand from Photovoltaic Cells and Wind Turbines—Investigating the Potential Risk of Disabling a Shift to Renewable Energy Systems,” *Science and Technology Options Assessment (STOA)*. Science and Technology Options Assessment (STOA), Brussel, Belgium, p. 72, 2012.
- [11] K. J. A. BBF Associates; Kundig, “Market study: Current and projected wind and solar renewable electric generating capacity and resulting copper demand.” Copper Development Association Inc., New York, U.S.A., 2011.
- [12] R. L. Moss, E. Tzimas, H. Kara, P. Willis, and J. Kooroshy, “Critical Metals in Strategic Energy Technologies, Assessing Rare Metals as Supply-Chain Bottlenecks in Low-Carbon Energy Technologies,” Publications Office of the European Union, Luxembourg, 2011.
- [13] J. L. Sullivan, C. E. Clarck, L. Yuan, J. Han, and M. Wang, “Life-Cycle Analysis Results for Geothermal Systems in Comparison to Other Power Systems: Part II,” Argonne, 2011.
- [14] I. A. S. Ehtiwind, M. C. Coelho, and A. C. M. Sousa, “Exergetic and environmental life cycle assessment analysis of concentrated solar power plants,” *Renew. Sustain. Energy Rev.*, vol. 56, pp. 145–155, Apr. 2016.
- [15] R. H. Crawford, “Life cycle energy and greenhouse emissions analysis of wind turbines and the effect of size on energy yield,” *Renew. Sustain. Energy Rev.*, vol. 13, no. 9, pp. 2653–2660, Dec. 2009.
- [16] R. Dones *et al.*, “Life Cycle Inventories of Energy Systems: Results for Current Systems in Switzerland and other UCTE Countries,” 2007.
- [17] K. R. Haapala and P. Prempreeda, “Comparative life cycle assessment of 2.0 MW wind turbines,” *Int. J. Sustain. Manuf.*, vol. 3, no. 2, p. 170, 2014.
- [18] A. Bonou, A. Laurent, and S. I. Olsen, “Life cycle assessment of onshore and offshore wind energy—from theory to application,” *Appl. Energy*, vol. 180, pp. 327–337, Oct. 2016.
- [19] C. Marimuthu and V. Kirubakaran, “Carbon pay back period for solar and wind energy project installed in India: A critical review,” *Renew. Sustain. Energy Rev.*, vol. 23, pp. 80–90, Jul. 2013.

- [20] B. Guezuraga, R. Zauner, and W. Pölz, "Life cycle assessment of two different 2 MW class wind turbines," *Renew. Energy*, vol. 37, no. 1, pp. 37–44, Jan. 2012.
- [21] K. Habib, "Critical Ressources in Clean Energy Technologies and Waste Flows," Syddansk Universitet, 2015.
- [22] D. R. Wilburn, "Wind energy in the United States and materials required for the land-based wind turbine industry from 2010 through 2030," in *Wind Turbine Manufacturing in the U.S.: Developments and Considerations*, 2012.
- [23] Energinet, "Technical Project Description for Offshore Wind Farms (200 MW)," Fredericia, 2015.
- [24] P. van Exter, S. Bosch, B. Schipper, B. Sprecher, and R. Kleijn, "Metal Demand for Renewable Electricity Generation in the Netherlands - Navigating a Complex Supply Chain," 2018.
- [25] Vici Ventus, "Offshore Wind Turbines: Concrete Foundations." Vici Ventus, Lysaker, 2020.
- [26] K. Flury and R. Frischknecht, "Life cycle inventories of hydroelectric power generation," *ESU-Services, Fair Consult. Sustain. Comm. by€ Oko-Institute eV*, pp. 1–51, 2012.
- [27] S&T2 consultants, "A Review of GHG emissions from Plant Construction and Decommissioning," Natural Resources Canada, Delta, Canada, 2006.
- [28] R. Dones, "Teil VII: Kernenergie," in *Sachbilanzen von Energiesystemen: Grundlagen fur den okologischen Vergleich von Energiesystemen und den Einbezug von Energiesystemen in Okobilanzen fur die Schweiz. Ecoinvent report No. 6*, R. et al. Dones, Ed. Dubendorf, Switzerland: Ecoinvent, 2007, p. 208.
- [29] J. P. Albers, W. J. Bawiec, L. F. Rooney, G. H. Goudarzi, and G. L. Shaffer, "Demand and Supply of Nonfuel Minerals and Materials for the United States Energy Industry, 1975–1990," 1977.
- [30] P. S. Weitzel, J. M. Tanzosh, B. Boring, N. Okita, T. Takahashi, and N. Ishikawa, "Advanced Ultra-Supercritical Power Plant (700 to 760C) Design for Indian Coal," 2012.
- [31] R. Dones, C. Bauer, and A. Roder, "Teil VI: Kohle," in *Sachbilanzen von Energiesystemen: Grundlagen fur den okologischen Vergleich von Energiesystemen und den Einbezug von Energiesystemen in Okobilanzen fur die Schweiz. Ecoinvent report No. 6*, R. et al. Dones, Ed. Dubendorf, Switzerland: Ecoinvent, 2007, p. 208.
- [32] B. Singh, E. A. Bouman, A. H. Strømman, and E. G. Hertwich, "Material use for electricity generation with carbon dioxide capture and storage: Extending life cycle analysis indices for material accounting," *Resour. Conserv. Recycl.*, vol. 100, pp. 49–57, Jul. 2015.
- [33] N. Jungbluth, "Teil IV: Erdöl," in *Sachbilanzen von Energiesystemen: Grundlagen fur den okologischen Vergleich von Energiesystemen und den Einbezug von Energiesystemen in Okobilanzen fur die Schweiz. Ecoinvent report No. 6*, R. Dones, Ed. Duebendorf: Swiss Centre for Life Cycle Inventories, 2007.
- [34] M. Faist-Emmenegger, T. Heck, N. Jungbluth, and M. Tuchschmid, "Teil V: Erdgas," in *Sachbilanzen von Energiesystemen: Grundlagen fur den okologischen Vergleich von Energiesystemen und den Einbezug von Energiesystemen in Okobilanzen fur die Schweiz. Ecoinvent report No. 6*, R. et al. Dones, Ed. Dubendorf, Switzerland: Ecoinvent, 2007, p. 208.
- [35] R. L. Moss *et al.*, "Critical metals in the path towards the decarbonisation of the EU energy sector," *Assessing rare metals as supply-chain bottlenecks in low-carbon energy technologies. JRC Report EUR*, vol. 25994. 2013.
- [36] C. Bauer, "Teil IX: Holzenergie," in *Sachbilanzen von Energiesystemen: Grundlagen fur den okologischen Vergleich von Energiesystemen und den Einbezug von Energiesystemen in Okobilanzen fur die Schweiz. Ecoinvent report No. 6*, R. et al. Dones, Ed. Dubendorf, Switzerland: Ecoinvent, 2007, p. 208.
- [37] Seneca Group, "Major Infrastructure Projects in Mexico - A Resource Guide for the U.S. Industry," Washington, 2014.
- [38] Eurelectric, "Power Distribution in Europe - Facts & Figures," Brussels, Belgium, 2013.
- [39] C. Arderne, C. Zorn, C. Nicolas, and E. E. Koks, "Predictive mapping of the global power system using open data," *Sci. Data*, vol. 7, no. 1, p. 19, Dec. 2020.
- [40] G. P. Harrison, E. (Ned). J. Maclean, S. Karamanlis, and L. F. Ochoa, "Life cycle assessment of the

- transmission network in Great Britain," *Energy Policy*, vol. 38, no. 7, pp. 3622–3631, Jul. 2010.
- [41] R. Turconi, C. G. Simonsen, I. P. Byriel, and T. Astrup, "Life cycle assessment of the Danish electricity distribution network," *Int. J. Life Cycle Assess.*, vol. 19, no. 1, pp. 100–108, Jan. 2014.
- [42] C. I. Jones and M. C. McManus, "Life-cycle assessment of 11kV electrical overhead lines and underground cables," *J. Clean. Prod.*, vol. 18, no. 14, pp. 1464–1477, Sep. 2010.
- [43] R. S. Jorge, T. R. Hawkins, and E. G. Hertwich, "Life cycle assessment of electricity transmission and distribution—part 2: transformers and substation equipment," *Int. J. Life Cycle Assess.*, vol. 17, no. 2, pp. 184–191, Feb. 2012.
- [44] R. S. Jorge, T. R. Hawkins, and E. G. Hertwich, "Life cycle assessment of electricity transmission and distribution—part 1: power lines and cables," *Int. J. Life Cycle Assess.*, vol. 17, no. 1, pp. 9–15, Jan. 2012.
- [45] F. Ueckerdt, R. Pietzcker, Y. Scholz, D. Stetter, A. Giannousakis, and G. Luderer, "Decarbonizing global power supply under region-specific consideration of challenges and options of integrating variable renewables in the REMIND model," *Energy Econ.*, vol. 64, pp. 665–684, May 2017.
- [46] M. Rogner and N. Troja, "The world's water battery: Pumped hydropower storage and the clean energy transition," London, 2018.
- [47] D. E. H. J. Gernaat, P. W. Bogaart, D. P. van Vuuren, H. Biemans, and R. Niessink, "High-resolution assessment of global technical and economic hydropower potential," *Nat. Energy*, vol. 2, no. 10, pp. 821–828, Oct. 2017.
- [48] B. Girod, D. P. van Vuuren, and S. Deetman, "Global travel within the 2 degree climate target," *Accept. to Energy Policy*, 2011.
- [49] L. Jian, H. Zechun, D. Banister, Z. Yongqiang, and W. Zhongying, "The future of energy storage shaped by electric vehicles: A perspective from China," *Energy*, vol. 154, pp. 249–257, Jul. 2018.
- [50] J. Geske and D. Schumann, "Willing to participate in vehicle-to-grid (V2G)? Why not!," *Energy Policy*, vol. 120, pp. 392–401, Sep. 2018.
- [51] IEA, "Tracking Clean Energy Progress 2017," Paris, 2017.
- [52] IRENA, *Electricity storage and renewables: Costs and markets to 2030*, no. October. 2017.
- [53] G. Majeau-Bettez, T. R. Hawkins, and A. H. Strømman, "Life Cycle Environmental Assessment of Lithium-Ion and Nickel Metal Hydride Batteries for Plug-In Hybrid and Battery Electric Vehicles," *Environ. Sci. Technol.*, vol. 45, no. 10, pp. 4548–4554, May 2011.
- [54] Wikipedia, "Nickel–metal hydride battery," 2019. [Online]. Available: https://en.wikipedia.org/wiki/Nickel–metal_hydride_battery. [Accessed: 25-Nov-2019].
- [55] Batteryuniversity.com, "Types of Lithium-ion," 2019. [Online]. Available: https://batteryuniversity.com/learn/article/types_of_lithium_ion. [Accessed: 25-Nov-2019].
- [56] H. Berg and M. Zackrisson, "Perspectives on environmental and cost assessment of lithium metal negative electrodes in electric vehicle traction batteries," *J. Power Sources*, vol. 415, pp. 83–90, Mar. 2019.
- [57] G. Xu, P. Han, S. Dong, H. Liu, G. Cui, and L. Chen, "Li 4 Ti 5 O 12 -based energy conversion and storage systems: Status and prospects," *Coord. Chem. Rev.*, vol. 343, pp. 139–184, Jul. 2017.
- [58] Y. Yang *et al.*, "Lithium Titanate Tailored by Cathodically Induced Graphene for an Ultrafast Lithium Ion Battery," *Adv. Funct. Mater.*, vol. 24, no. 27, pp. 4349–4356, Jul. 2014.
- [59] T. M. Gür, "Review of electrical energy storage technologies, materials and systems: challenges and prospects for large-scale grid storage," *Energy Environ. Sci.*, vol. 11, no. 10, pp. 2696–2767, 2018.
- [60] P. Van den Bossche, J. Matheys, and J. Van Mierlo, "Battery Environmental Analysis," in *Electric and Hybrid Vehicles*, Elsevier, 2010, pp. 347–374.
- [61] C. J. Rydh, "Environmental assessment of vanadium redox and lead-acid batteries for stationary energy storage," *J. Power Sources*, vol. 80, no. 1–2, pp. 21–29, Jul. 1999.

- [62] Batteryuniversity.com, "Why does Sodium-sulfur need to be heated," 2019. [Online]. Available: https://batteryuniversity.com/learn/article/bu_210a_why_does_sodium_sulfur_need_to_be_heated. [Accessed: 25-Nov-2019].
- [63] G. Li *et al.*, "Advanced intermediate temperature sodium–nickel chloride batteries with ultra-high energy density," *Nat. Commun.*, vol. 7, no. 1, p. 10683, Apr. 2016.
- [64] K. Patel, "Lithium-Sulfur Battery: Chemistry, Challenges, Cost, and Future," *J. Undergrad. Res. Univ. Illinois Chicago*, vol. 9, no. 2, Aug. 2016.
- [65] Y. Deng, J. Li, T. Li, X. Gao, and C. Yuan, "Life cycle assessment of lithium sulfur battery for electric vehicles," *J. Power Sources*, vol. 343, pp. 284–295, Mar. 2017.
- [66] S. Yu *et al.*, "Insights into a layered hybrid solid electrolyte and its application in long lifespan high-voltage all-solid-state lithium batteries," *J. Mater. Chem. A*, vol. 7, no. 8, pp. 3882–3894, 2019.
- [67] P. Albertus, S. Babinec, S. Litzelman, and A. Newman, "Status and challenges in enabling the lithium metal electrode for high-energy and low-cost rechargeable batteries," *Nat. Energy*, vol. 3, no. 1, pp. 16–21, Jan. 2018.
- [68] B. Collins and BloombergNEF, "Innolith Battery Strikes at 'Flammable' Lithium-Ion: Q&A," 2019.
- [69] S. J. Gerssen-Gondelach and A. P. C. Faaij, "Performance of batteries for electric vehicles on short and longer term," *J. Power Sources*, vol. 212, pp. 111–129, Aug. 2012.
- [70] M. Zackrisson, K. Fransson, J. Hildenbrand, G. Lampic, and C. O'Dwyer, "Life cycle assessment of lithium-air battery cells," *J. Clean. Prod.*, vol. 135, pp. 299–311, Nov. 2016.
- [71] P. Tan *et al.*, "Advances and challenges in lithium-air batteries," *Appl. Energy*, vol. 204, pp. 780–806, Oct. 2017.
- [72] Z. Zhu *et al.*, "Anion-redox nanolithia cathodes for Li-ion batteries," *Nat. Energy*, vol. 1, no. 8, p. 16111, Aug. 2016.
- [73] K. G. Gallagher *et al.*, "Quantifying the promise of lithium–air batteries for electric vehicles," *Energy Environ. Sci.*, vol. 7, no. 5, p. 1555, 2014.
- [74] X. Luo, J. Wang, M. Dooner, and J. Clarke, "Overview of current development in electrical energy storage technologies and the application potential in power system operation," *Appl. Energy*, vol. 137, pp. 511–536, Jan. 2015.
- [75] M. R. Gardiner, "Hydrogen for Energy Storage," *Presentation*, 2014. [Online]. Available: <https://www.h2fc-fair.com/hm14/images/tech-forum-presentations/2014-04-09-1700.pdf>.
- [76] M. A. Cusenza, S. Bobba, F. Ardente, M. Cellura, and F. Di Persio, "Energy and environmental assessment of a traction lithium-ion battery pack for plug-in hybrid electric vehicles," *J. Clean. Prod.*, vol. 215, pp. 634–649, Apr. 2019.
- [77] P. A. Nelson, S. Ahmed, K. G. Gallagher, and D. W. Dees, "Modeling the Performance and Cost of Lithium-Ion Batteries for Electric-Drive Vehicles," Argonne, 2019.
- [78] Dakota Lithium, "Safety Data Sheet Lithium Phosphate (LiFePO₄)."
- [79] Y. Olofsson and M. Romare, "Life Cycle Assessment of Lithium-ion Batteries for Plug-in Hybrid Buses," Chalmers University of Technology, Sweden, 2013.
- [80] C. Chen, R. Agrawal, and C. Wang, "High Performance Li₄Ti₅O₁₂/Si Composite Anodes for Li-Ion Batteries," *Nanomaterials*, vol. 5, no. 3, pp. 1469–1480, Aug. 2015.
- [81] J. L. Sullivan and L. Gaines, "A Review of Battery Life-Cycle Analysis: State of Knowledge and Critical Needs," Argonne, 2010.
- [82] Axpo, "Environmental Product declaration Löntsch high head storage power plant," Baden, 2018.
- [83] A. Eller, I. McClanney, and De. Gauntlett, "North American Energy Storage Copper Content Analysis," 2018.
- [84] K. Liu and X.-G. Chen, "Development of Al–Mn–Mg 3004 alloy for applications at elevated temperature via

dispersoid strengthening," *Mater. Des.*, vol. 84, pp. 340–350, Nov. 2015.

- [85] Azo Materials, "AISI 4340 Alloy Steel (UNS G43400)," 2020. [Online]. Available: <https://www.azom.com/article.aspx?ArticleID=6772>. [Accessed: 19-May-2020].
- [86] F. N. Werfel *et al.*, "250 kW flywheel with HTS magnetic bearing for industrial use," *J. Phys. Conf. Ser.*, vol. 97, p. 012206, Feb. 2008.
- [87] S. Deetman, S. Marinova, E. van der Voet, D. P. van Vuuren, O. Edelenbosch, and R. Heijungs, "Modelling global material stocks and flows for residential and service sector buildings towards 2050," *J. Clean. Prod.*, vol. 245, 2020.
- [88] O. Koskinen and C. Breyer, "Energy Storage in Global and Transcontinental Energy Scenarios: A Critical Review," *Energy Procedia*, vol. 99, pp. 53–63, 2016.
- [89] G. A. H. Laugs, R. M. J. Benders, and H. C. Moll, "Balancing responsibilities: Effects of growth of variable renewable energy, storage, and undue grid interaction," *Energy Policy*, vol. 139, p. 111203, 2020.
- [90] M. Child, C. Kemfert, D. Bogdanov, and C. Breyer, "Flexible electricity generation, grid exchange and storage for the transition to a 100% renewable energy system in Europe," *Renew. Energy*, vol. 139, pp. 80–101, 2019.
- [91] S. Chatzivasileiadis, D. Ernst, and G. Andersson, "The Global Grid," *Renew. Energy*, vol. 57, pp. 372–383, 2013.
- [92] A. F. Hof *et al.*, "From global to national scenarios: Bridging different models to explore power generation decarbonisation based on insights from socio-technical transition case studies," *Technol. Forecast. Soc. Change*, vol. 151, p. 119882, Feb. 2020.
- [93] P. Berrill, A. Arvesen, Y. Scholz, H. C. Gils, and E. G. Hertwich, "Environmental impacts of high penetration renewable energy scenarios for Europe," *Environ. Res. Lett.*, vol. 11, no. 1, p. 014012, Jan. 2016.
- [94] W. Li, S. Lee, and A. Manthiram, "High-Nickel NMA: A Cobalt-Free Alternative to NMC and NCA Cathodes for Lithium-Ion Batteries," *Adv. Mater.*, vol. 32, no. 33, p. 2002718, Aug. 2020.
- [95] M. O. Reese *et al.*, "Increasing markets and decreasing package weight for high-specific-power photovoltaics," *Nat. Energy*, vol. 3, no. 11, pp. 1002–1012, Nov. 2018.
- [96] A. Lefevre, S. Garnier, L. Jacquemin, B. Pillain, and G. Sonnemann, "Anticipating in-use stocks of carbon fibre reinforced polymers and related waste generated by the wind power sector until 2050," *Resour. Conserv. Recycl.*, vol. 141, pp. 30–39, Feb. 2019.
- [97] P. Steen, P. Landel, E. Dölerud, and Otto Lundman, "Structural design methods for tall timber towers with large wind turbine," in *International Conference on Computational Methods in Wood Mechanics*, 2019, p. 27.